MSUCP-9

MICHIGAN STATE UNIVERSITY

CYCLOTRON PROJECT*

Computational Study of Factors Determining the Optical Characteristics of a Resonant Extraction System for a 3 Sector Cyclotron

H. G. Blosser and M. M. Gordon

January 1961

Department of Physics

East Lansing, Michigan

*Research Supported in part by U. S. Atomic Energy Commission Contract AT(11-1)-872

I. INTRODUCTION

One of the important performance attributes of an ion optical system is the character and extent of the distortions and aberrations which the system imposes on the transmitted beam. Resonant extraction in a medium energy 3 sector cyclotron utilizes a non-linear phenomena, the 3/3 resonance, to generate turn separation; any such non-linear effect is per se a likely source of distortion and aberration. This report presents results of a series of studies at MSU of the optical characteristics of such an extraction system. The study is restricted to consideration of the median plane characteristics of the motion.[1.]

---

1. Off median plane trajectories will undoubtedly display some additional aberrations. It is believed that these are in general small compared to the median plane effects, since the small axial beam space in a cyclotron constrains the particles to move in a region where the z dependence of the field is quite linear. Results from a few trial runs are in accord with this expectation.

The studies are accomplished by orbit tracking using a series of computer routines to accomplish numerical integrations of the equations of motion. Magnetic field data are derived from model magnet studies. The results herein reported are for a magnetic field configuration, designated B26.1R, arrived at in an early stage of the MSU studies; a number of changes in the field configuration leading to various performance improvements have since been arrived at. It is nevertheless deemed worthwhile to make a detailed presentation of the B26.1R results since:

1) the field has been studied in considerably more detail than any of the subsequent modifications,

2) the detailed computational results for this field deliniate with considerable clarity the basic factors determining

the optical characteristics of the system -- these factors are of general applicability.

3) by presenting the B26.1R results, subsequent presentations of the more meager results for other fields will be easier to understand.

II. CALCULATION PROCEDURES

A study of the optical characteristics of a resonant extraction process must include acceleration effects since the behavior, as will be seen in following results, is quite sensitive to the rate of acceleration. Direct consideration of accelerated orbits, and phase plots is not however an easy way to ascertain and understand the field features responsible for particular orbit characteristics. Fortunately, in most of a cyclotron, the acceleration can be considered to good approximation as being a simple impulsive change in the energy of the particle at the azimuth of the accelerating gap, followed by a coasting or static trajectory to the azimuth of the next gap. Coasting in the median plane from one acceleration gap to the next, can be viewed as a two dimensional mapping process, the features of which are given by the static r, p_r phase plot for the particular energy. At the gap crossing the energy changes, therefore changing the applicable phase plot -- thereafter the process repeats. Since the features of the phase plots change in a continuous way as the energy changes, the features of the mapping at any energy can be inferred by interpolation in a set of plots at a few energies covering the range of interest. Behavior of the static phase plots can in turn be related fairly directly to particular features of the magnetic field. In the computations, both static and accelerated orbit behavior have therefore been studied; by considering the results of the two types of study in combination, a thorough understanding of the process can be achieved.

As in MSUCP-6 orbit computations are made using the Fixed Point Code[2]. and the General Orbit Code[3]. for the MSU

---

2. T. I. Arnette, M. M. Gordon, and H. G. Blosser, MSUCP report in preparation.

3. M. M. Gordon and H. G. Blosser, Mistic General Orbit Code MSUCP-7 (1960) unpublished.

---

computer, the Mistic. The Fixed Point Code locates closed orbits by means of a highly effective linear transfer matrix procedure, the General Orbit Code tracks arbitrary orbits as desired either with or without acceleration effects. For both routines the magnetic field is described by tables of Fourier coeffecients as functions of radius; each uses equations of motion which are exact in the median plane.

To deliniate the features of the static phase plot for some energy, the fixed point routine is first employed to locate the various closed orbits (occasionally for expediency only the unstable fixed points are located) after which the general orbit code is employed to trace forward and backward in time orbits with initial conditions displaced slightly from the unstable fixed points. These orbits to good approximation represent the boundaries of the various topological regions of the plot which are the principal feature of interest.

To ascertain more accurately the extent of aberrative effects in various regions of the plot, additional orbits are traced as needed.

For a cyclotron with two accelerating gaps per revolution the mapping function of direct interest is that for a half turn -- for magnetic fields, such as the one considered here which do not have 180° periodicity, this mapping cannot be expressed in terms of a phase plot. The composite of the mappings thru a pair of half turns is however approximately

equivalent to the static mapping for a whole turn. If, in the interpretation, a correction factor is included as described in Section IV to account for the shift in fixed point locations at the gap crossing, the accelerated full revolution mapping (comprising half revolution, gap crossing, half revolution) can be inferred quite accurately from the static full revolution mapping. In view of this and of the great ease of presentation of the static full revolution mapping as a phase plot, all non-accelerated orbit results are presented as once per revolution static phase plots.

The B26.1R magnetic field is given in Table I. The field is derived from a model magnet study known as Run 26 [4]. with

---

4. H. G. Blosser and D. A. Flanigan, Run 26 Field Information, MSUCP-3 (1960), unpublished.

---

modifications to <B> to yield isochronism out to the 29th entry in the radial table and with the flutter field modified by a small amount to smooth out effects of measurement errors. In addition, Fourier components of argument greater than 9θ have been dropped since these components are sufficiently small to have a negligible effect on the particle motion. The radial spacing of the table entrys is interpreted as increased by the factor 64/8.75 corresponding to the ratio of pole diameters of the proposed MSU cyclotron and the Run 26 magnet. For protons the radial separation in cyclotron units between successive entrys in the field table, then becomes 0.0080924.

In the Fourier analysis the measured field has been assumed to have perfect 120° symmetry. To accomplish extraction at a single azimuth an additional field component with once per revolution symmetry must be added. This component, called the "field bump", has the form $B(r,\theta) = B_1(r)\cos(\theta + 2.8°)$ for the runs herein described. The function $B_1(r)$ is given in Table II, the radial profile corresponding to the shape expected from the "bump coil" geometry employed in the MSU cyclotron design.

r MODEL INCHES	B_o GAUSS	H_3 GAUSS	G_3 GAUSS	H_6 GAUSS	G_6 GAUSS	H_9 GAUSS	G_9 GAUSS
0.1	+13623	+00025	-00004	-00019	-00019	+00008	-00030
0.2	+13624	+00060	-00100	+00018	+00027	+00000	+00005
0.3	+13625	+00187	-00302	+00023	+00045	-00006	+00009
0.4	+13624	+00378	-00570	+00010	+00043	-00009	-00003
0.5	+13620	+00612	-00872	-00009	+00026	-00007	-00023
0.6	+13614	+00875	-01185	-00027	+00002	+00000	-00042
0.7	+13607	+01159	-01488	-00041	-00025	+00012	-00053
0.8	+13600	+01457	-01768	-00047	-00052	+00028	-00053
0.9	+13593	+01766	-02016	-00047	-00074	+00046	-00040
1.0	+13587	+02081	-02227	-00042	-00089	+00065	-00013
1.1	+13583	+02395	-02399	-00035	-00095	+00084	+00026
1.2	+13579	+02706	-02531	-00028	-00091	+00100	+00077
1.3	+13578	+03007	-02624	-00027	-00077	+00111	+00136
1.4	+13578	+03296	-02682	-00032	-00052	+00116	+00201
1.5	+13580	+03570	-02708	-00047	-00017	+00113	+00268
1.6	+13587	+03825	-02703	-00073	+00028	+00102	+00333
1.7	+13601	+04062	-02672	-00111	+00080	+00081	+00395
1.8	+13617	+04280	-02618	-00161	+00139	+00052	+00450
1.9	+13634	+04479	-02544	-00222	+00202	+00015	+00496
2.0	+13651	+04660	-02452	-00295	+00266	-00029	+00531
2.1	+13669	+04823	-02347	-00379	+00330	-00078	+00556
2.2	+13690	+04968	-02232	-00471	+00390	-00130	+00570
2.3	+13714	+05097	-02107	-00571	+00445	-00183	+00572
2.4	+13737	+05207	-01977	-00678	+00491	-00233	+00564
2.5	+13761	+05300	-01842	-00790	+00527	-00278	+00546
2.6	+13792	+05376	-01704	-00905	+00550	-00316	+00520
2.7	+13827	+05434	-01564	-01022	+00558	-00345	+00486
2.8	+13861	+05476	-01422	-01140	+00551	-00363	+00447
2.9	+13890	+05505	-01278	-01258	+00528	-00368	+00404
3.0	+13907	+05523	-01133	-01374	+00488	-00359	+00358
3.1	+13917	+05534	-00987	-01486	+00432	-00337	+00313
3.2	+13918	+05541	-00840	-01593	+00362	-00301	+00268
3.3	+13911	+05545	-00693	-01693	+00278	-00253	+00227
3.4	+13895	+05545	-00547	-01783	+00186	-00197	+00191
3.5	+13864	+05538	-00404	-01859	+00087	-00133	+00160
3.6	+13805	+05517	-00265	-01919	-00013	-00068	+00137
3.7	+13709	+05471	-00135	-01959	-00110	-00004	+00121
3.8	+13564	+05386	-00016	-01973	-00199	+00054	+00114
3.9	+13352	+05249	+00085	-01958	-00276	+00104	+00114
4.0	+13046	+05046	+00166	-01909	-00337	+00141	+00120
4.1	+12608	+04765	+00223	-01824	-00379	+00164	+00132
4.2	+12001	+04396	+00252	-01701	-00399	+00172	+00147
4.3	+11231	+03935	+00255	-01542	-00396	+00166	+00161
4.4	+10343	+03390	+00234	-01352	-00371	+00148	+00171
4.5	+09408	+02785	+00194	-01139	-00326	+00123	+00171
4.6	+08497	+02172	+00146	-00917	-00265	+00098	+00155
4.7	+07661	+01640	+00102	-00704	-00195	+00083	+00115
4.8	+06930	+01317	+00083	-00525	-00123	+00090	+00044

TABLE I: TABLES GIVING FIELD COEFFICIENTS VS. RADIUS. IN THE CALCULATIONS RADIAL SPACING IS INTERPRETED AS INCREASED BY FACTOR 64/8.75 RESULTING IN RADIAL INCREMENT IN CYCLOTRON UNITS OF 0.0080924.

$$B(r, \theta) = Bo(r) + \sum_{j=1}^{3} (H_{3j} \cos 3j\theta + G_{3j} \sin 3j\theta)$$

r MODEL INCHES	B_1 GAUSS
0.1	00000
0.2	00000
0.3	00000
0.4	00000
0.5	00000
0.6	00000
0.7	00000
0.8	00000
0.9	00000
1.0	00000
1.1	00000
1.2	00000
1.3	00000
1.4	00000
1.5	00000
1.6	00000
1.7	00000
1.8	00000
1.9	00000
2.0	00000
2.1	00001
2.2	00002
2.3	00004
2.4	00009
2.5	00014
2.6	00022
2.7	00034
2.8	00053
2.9	00080
3.0	00109
3.1	00131
3.2	00139
3.3	00131
3.4	00109
3.5	00080
3.6	00053
3.7	00034
3.8	00022
3.9	00014
4.0	00009
4.1	00004
4.2	00002
4.3	00001
4.4	00000
4.5	00000
4.6	00000
4.7	00000
4.8	00000

TABLE II: AMPLITUDE OF COS θ FIELD COMPONENT VS. RADIUS.

Properties of static orbits in the B26.1R field have been studied both with and without the field bump, and results of both are included herein. When the above bump is included in the field an extra 1 is added to the field number i.e. B26.1R with bump is B26.11R.

III. STATIC ORBIT RESULTS

Fig 1 is a static r, p_r phase plot at azimuth $\theta = 0$ for a group of trajectories in the pure 3 sector or "unbumped" field, the coasting particle being in each case a proton of energy 28 Mev. As in all the phase plots in this report the radius is given in cyclotron units, where 1 cyc. unit = E_o/qB_oc (in mks units) with E_o the rest energy of the accelerated particle, q the charge of the accelerated particle, B_o the value of the magnetic field at r = o, and c the velocity of light. The radial component of momentum is plotted in units of m_oc. The phase plot is obtained by starting a trajectory from some assigned initial conditions (r, p_r) at $\theta = 0$ tracking for some number of revolutions, and plotting r, p_r each time the trajectory passes $\theta = 0$. Successive such points from a given trajectory are joined by a line. Arrows on the phase plot lines indicate the direction of evolution of the points for particles rotating in the negative θ direction i.e. magnetic field in positive Z direction.

As is familiar, the phase space looking at Fig. 1, is seen to be divided into five clearly distinct regions, (1) the central triangular region, (2) (3) (4) the three outer oval shaped regions at right, upper left and lower left of the figure, and (5) the exterior surrounding the four already mentioned regions. At the centers of each of the four closed regions and at the three boundary intersections, "fixed points" are found i.e. points with the unique property that an orbit started with these initial conditions will continue indefinitely to return to the same (r, p_r) on each subsequent revolution. Location of the seven fixed points to a large extent determines the features of the phase plot.

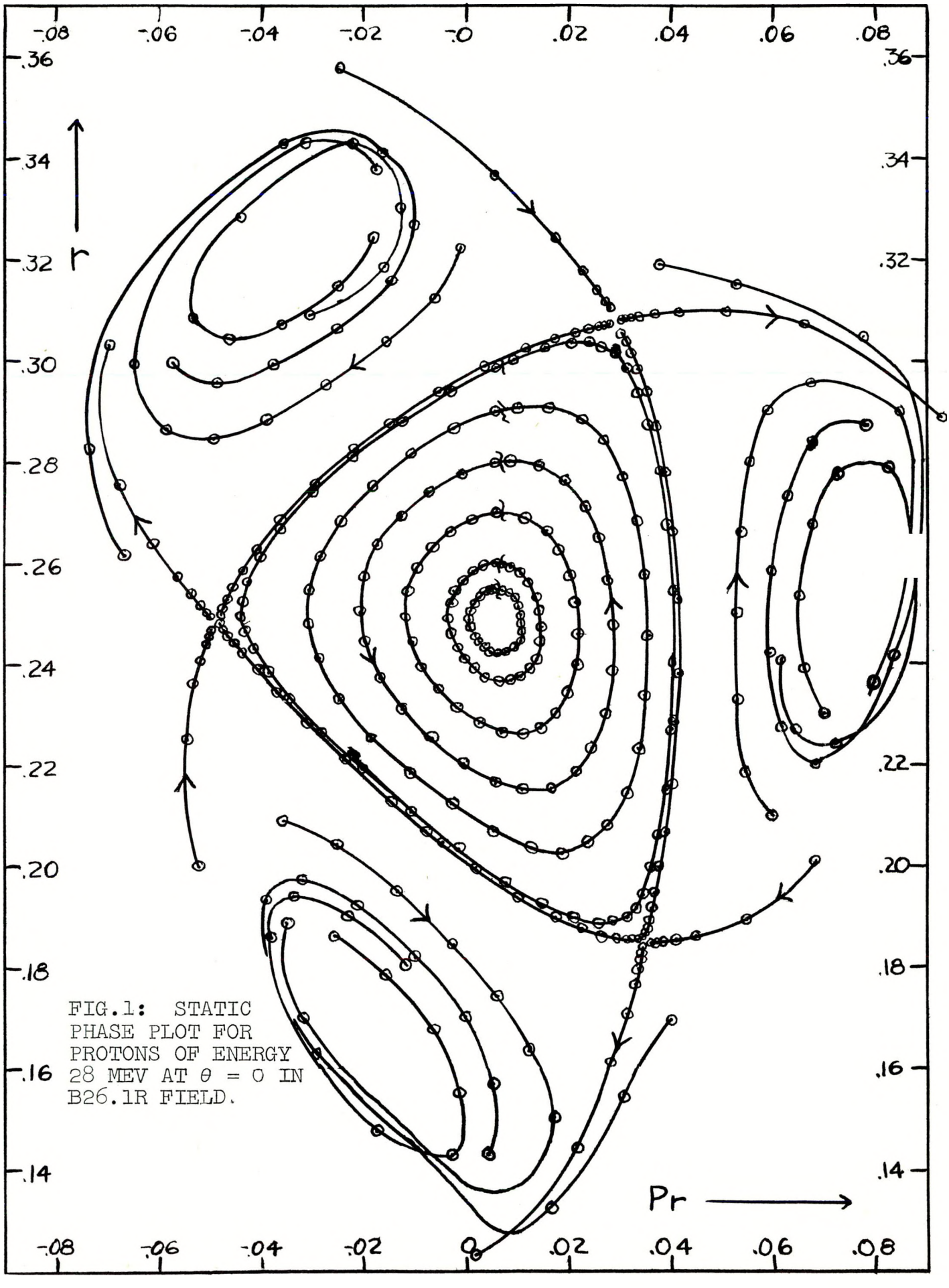

FIG.1: STATIC PHASE PLOT FOR PROTONS OF ENERGY 28 MEV AT θ = 0 IN B26.1R FIELD.

Fig. 2 is an (r, p_r) plot for the unbumped field, showing the positions of the various fixed points at a number of energies. Curves on this graph now connect positions of a particular fixed point at various energies. For many of the points the energies are specifically labeled -- where the energies are not labeled, points between labeled points are uniformly spaced in energy between the labeled values, i.e. on the S3 curve, the three unlabeled points between labeled points 24 and 28 are at energies of 25, 26, and 27 Mev respectively, etc. By comparison with Fig. 1 it is seen that the curve labeled E.O. marks the successive positions of the center of the stable triangle (the "equilibrium"orbit), the curves marked U1, U2, and U3 mark the boundary intersection points and the curves marked S1, S2, and S3 are the central closed orbits of the three outer regions.

To aid in relating orbits and field features the seven closed orbits for a particle of energy 30 Mev have been plotted on a polar graph and are shown in Fig. 3 superimposed on an approximate contour map for the B26.1R field (the contour map is actually for the Run 26 field but differs only slightly from B26.1R field values). The equilibrium orbit is centered about the machine center, the outer stable orbits are seen to hang over the edge of one of the hills and the unstable fixed point orbits are a bounding situation. Fig. 4 is a similar polar plot except in this case only the S1 fixed point orbit has been plotted but at six different energies. From the figure the S1 fixed point is seen to correspond to a family of closed orbits which at low energies are approximately centered about the peak of one of the "hills" of the field and which grow with energy. S2 and S3 would correspond to similar families originating on the other two hills.

Referring again to Fig. 2 note that as the energy increases all of the fixed points move closer together as is qualitatively reasonable since the field is of limited spatial extent and all of the orbits grow as the energy grows. At an energy of about

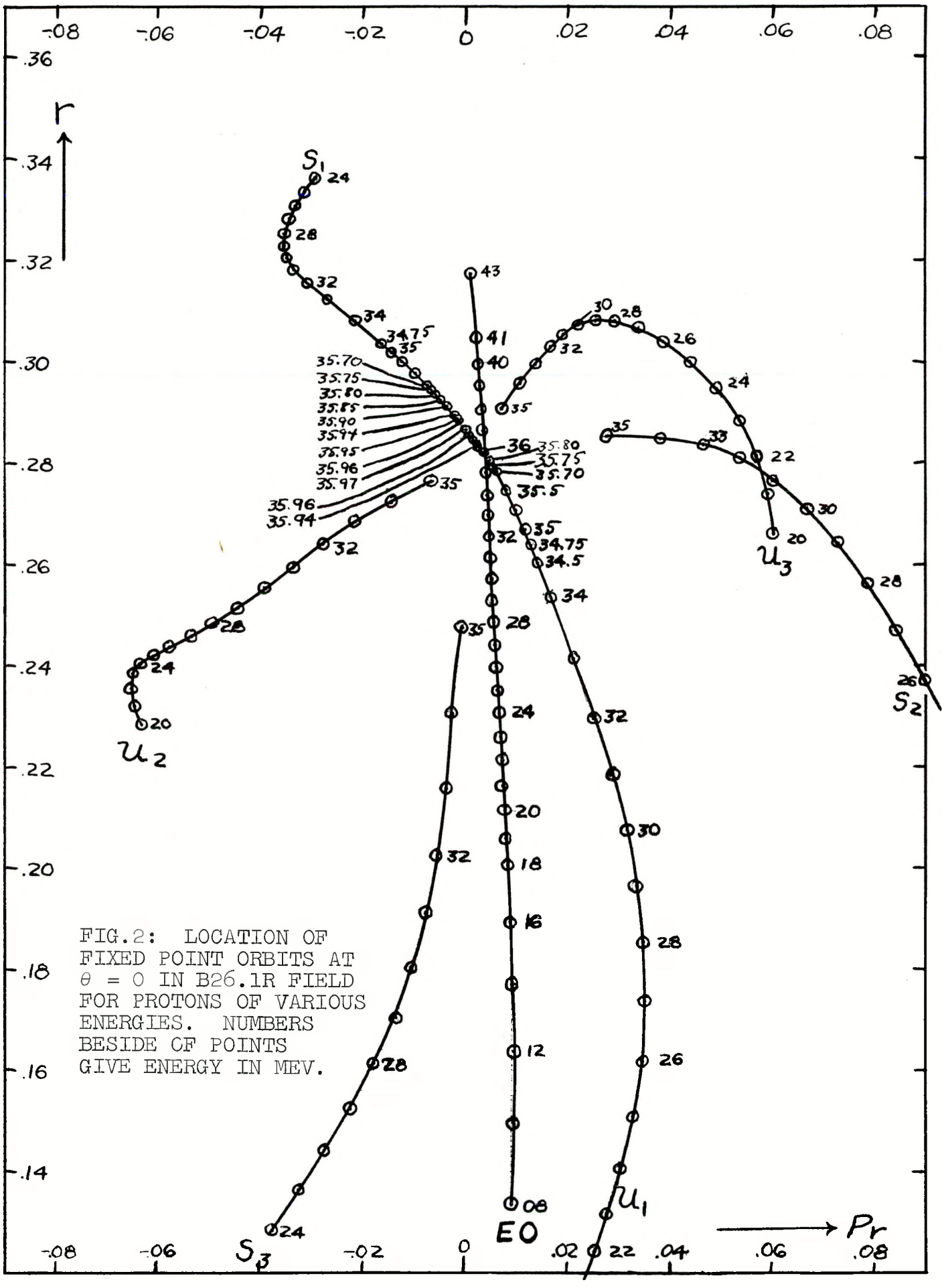

FIG.2: LOCATION OF FIXED POINT ORBITS AT $\theta = 0$ IN B26.1R FIELD FOR PROTONS OF VARIOUS ENERGIES. NUMBERS BESIDE OF POINTS GIVE ENERGY IN MEV.

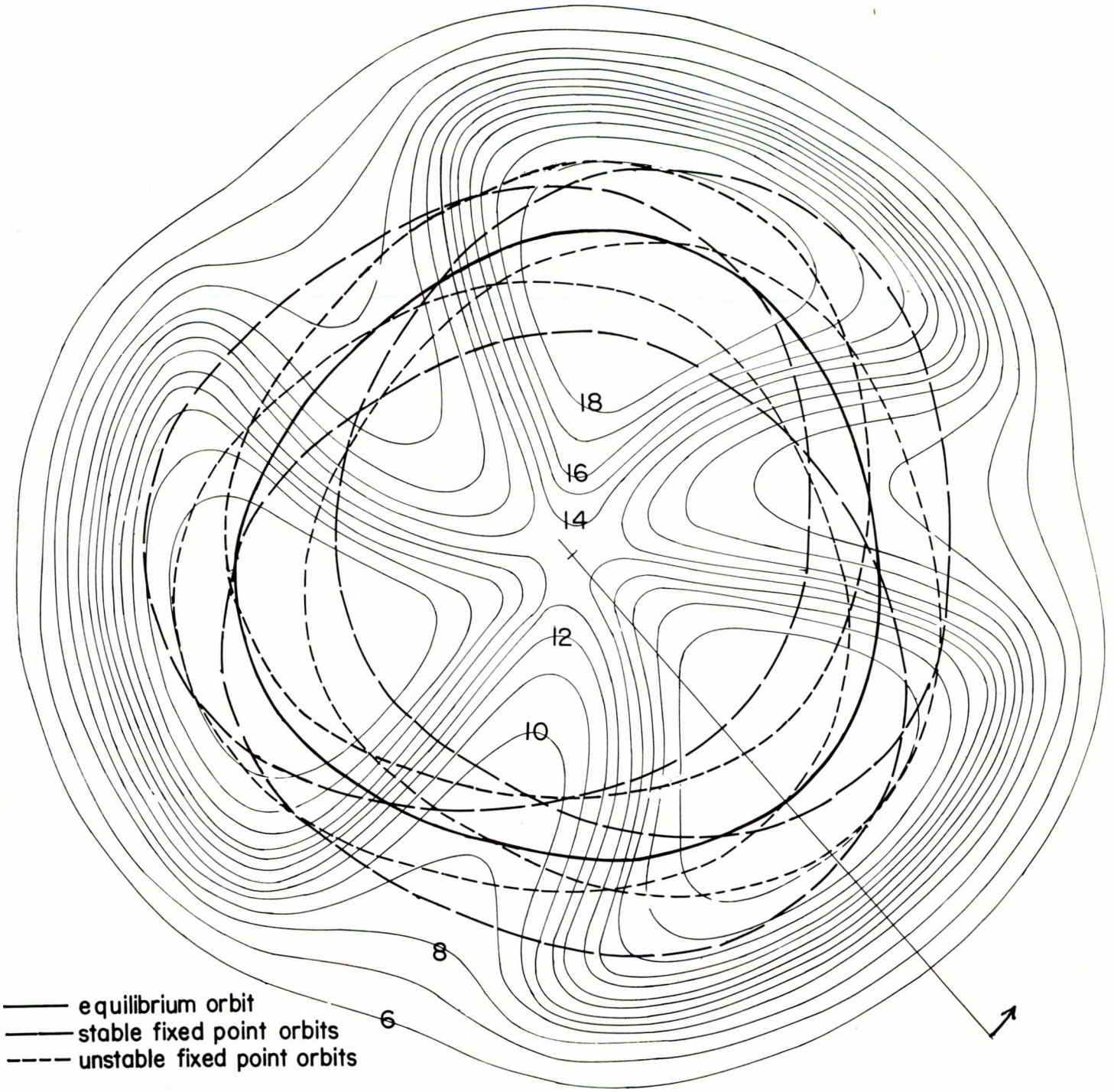

FIG.3: POLAR PLOT OF SEVEN FIXED POINT ORBITS FOR 30 MEV PROTONS IN B26.1R FIELD, SUPERIMPOSED ON CONTOUR MAP OF RUN 26 FIELD. RADIAL LINE MARKS $\theta = 0$; FORWARD ROTATION IS IN DIRECTION OF ARROW, WHICH IS ALSO NEGATIVE θ DIRECTION (CONTOUR MAP IS AN INVERTED IMAGE). NUMBERS ON CONTOURS GIVE FIELD STRENGTH IN KILOGAUSS.

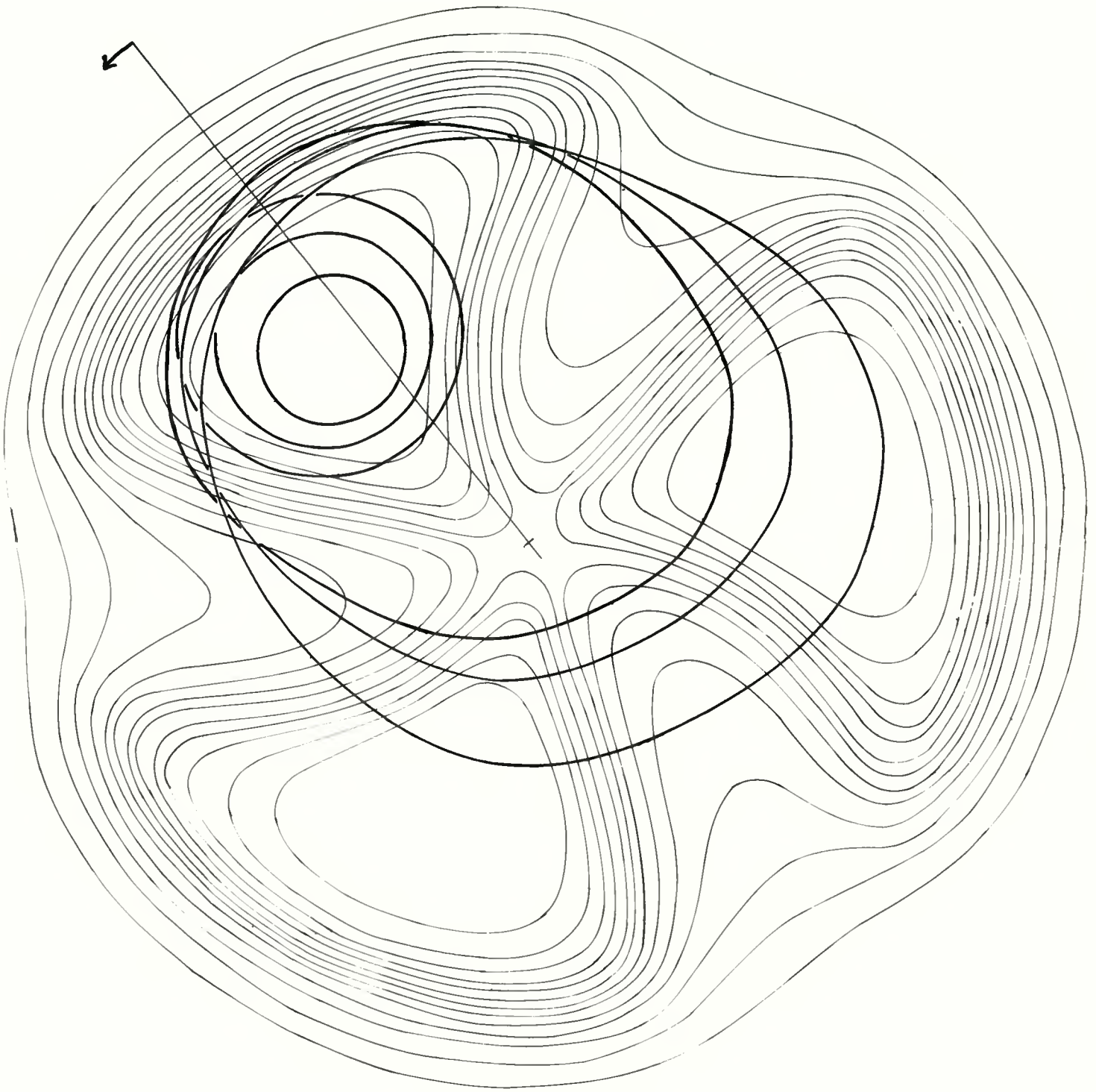

FIG.4: POLAR PLOT OF S1 FIXED POINT ORBIT FOR PROTONS OF ENERGIES 3, 6, 9, 18, 22, AND 30 MEV, SUPERIMPOSED ON CONTOUR MAP OF RUN 26 FIELD. RADIAL LINE MARKS θ = 0; FORWARD ROTATION IS IN DIRECTION OF ARROW.

35.85 Mev, the U1 curve is seen to cross the E.O. curve and U2 and U3 would do the same except that for clarity the U2 and U3 results have not been plotted. The crossing implies several things: (1) the E.O. U1, U2, and U3 fixed point orbits all coincide, (2) the central triangle has shrunk to zero size, and (3) the small amplitude focusing frequency ν_r has shifted to the resonant value unity. At higher energies U1 moves away from E0 on the opposite side corresponding to an inversion of the stable triangle and with the small amplitude ν_r less than unity. This condition persists only for a narrow band of energies. At roughly 35.97 Mev U1 and S1 meet and disappear corresponding to the shrinking and vanishing of the outer stable regions of the phase plot. At higher energies only the single E.O. fixed point remains, corresponding to a large centered orbit if plotted on the field contour map.

Figs. 5, 6, 7, 8, and 9 are a succession of static phase plots analagous to Fig. 1 but with successively increased particle energies. Most of the features surmised from Fig. 2 are evidenced in the actual phase plots. The principal feature not displayed is the inversion of the stable triangle which occurs between 35.85 and 35.97 Mev. In this energy range, due to the proximity of $\nu_r = 1$, motion of points on the phase diagram is so slow that an exorbitant amount of computation would be required to actually exhibit the inverted triangle (the innermost curve in Fig. 8 for example represents 295 revolutions). Moreover in view of the fixed point code results of Fig. 2, the inverted triangle is assuredly there, so little purpose is served in actually displaying it.

When the bump is added to the field, marked shifts in the phase plot features occur in accord with predictions of simplified treatments of the process.[5] Fig. 10 shows the

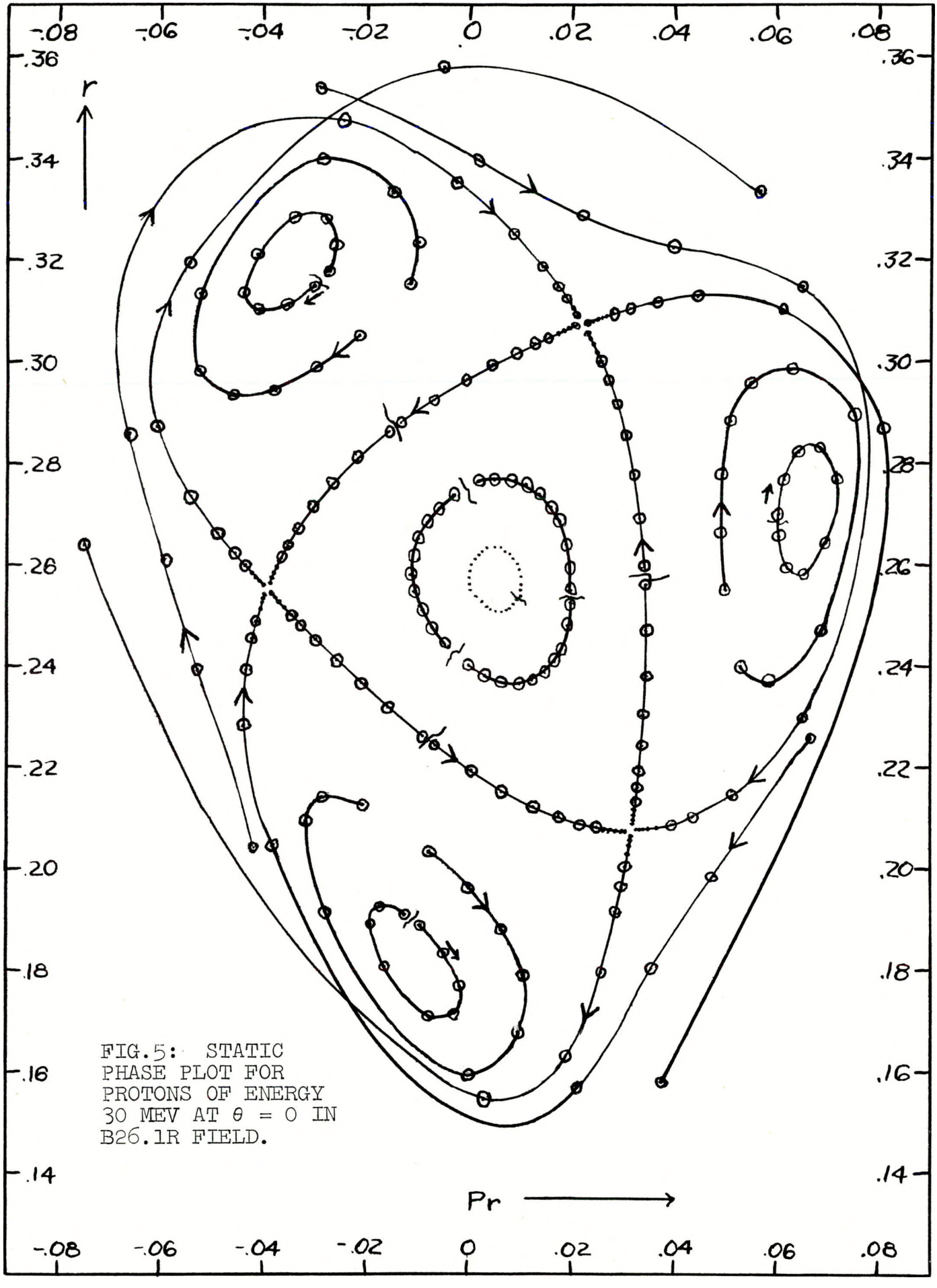

FIG.5: STATIC PHASE PLOT FOR PROTONS OF ENERGY 30 MEV AT θ = 0 IN B26.1R FIELD.

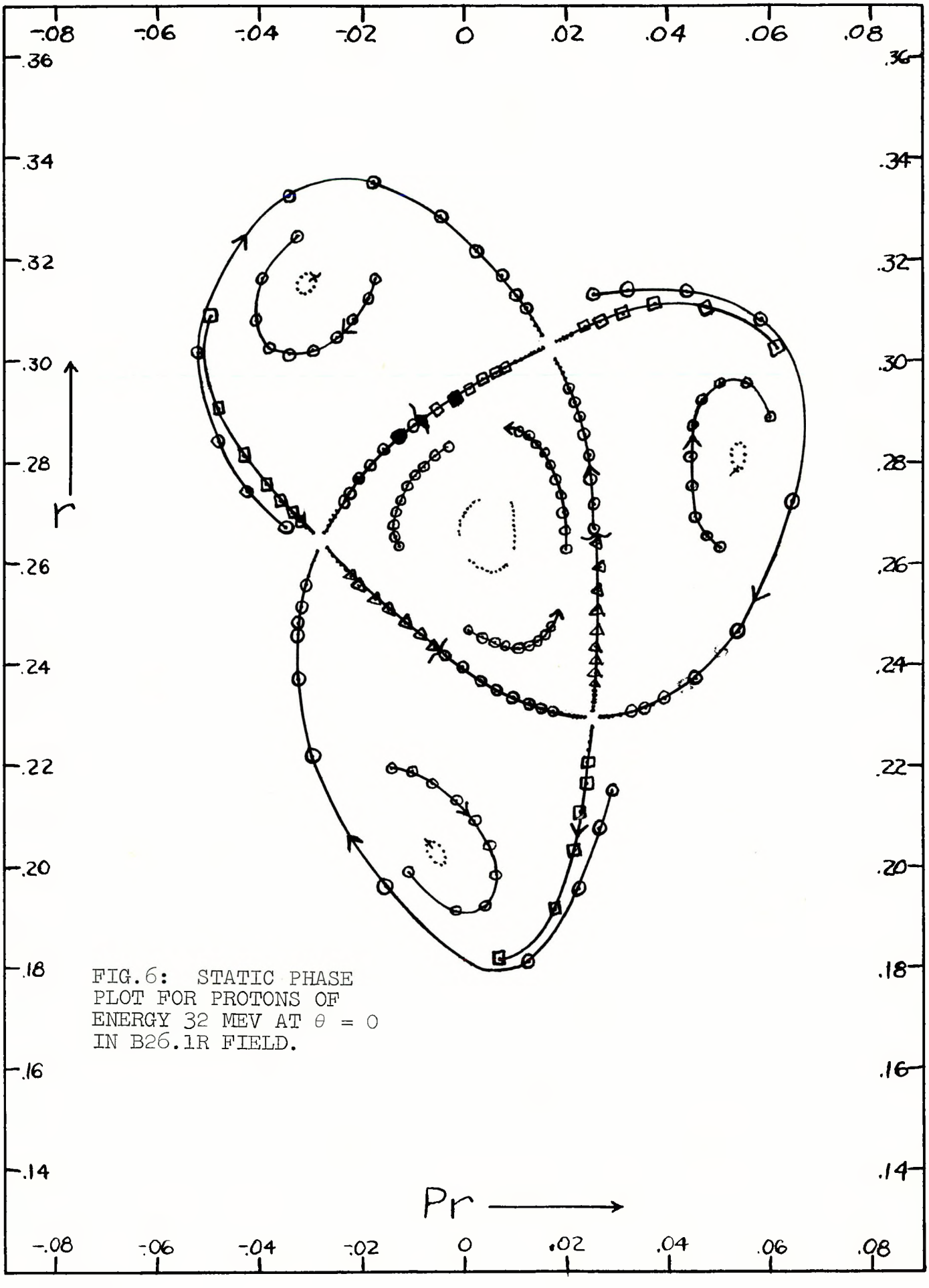

FIG.6: STATIC PHASE PLOT FOR PROTONS OF ENERGY 32 MEV AT $\theta = 0$ IN B26.1R FIELD.

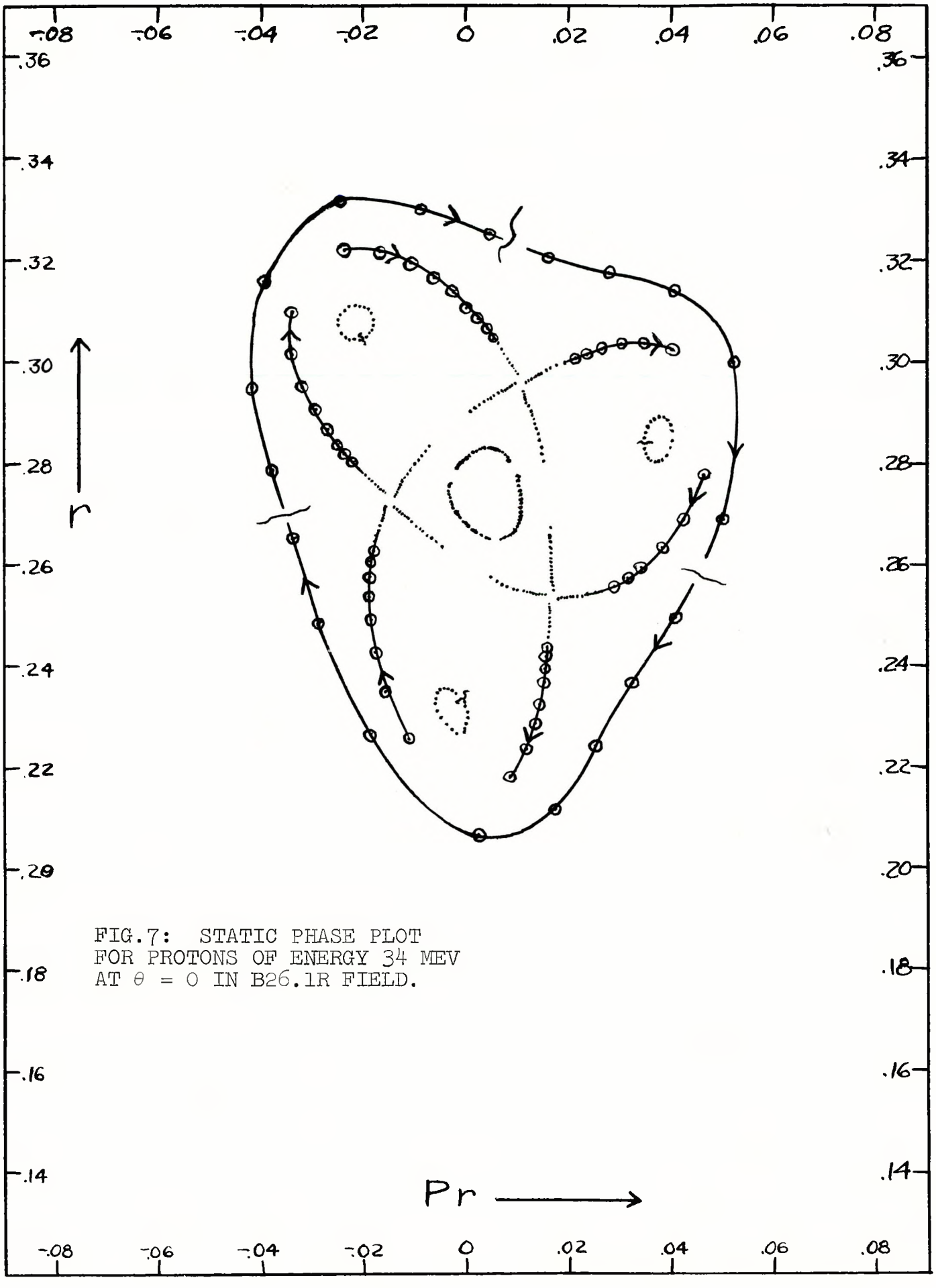

FIG.7: STATIC PHASE PLOT
FOR PROTONS OF ENERGY 34 MEV
AT θ = 0 IN B26.1R FIELD.

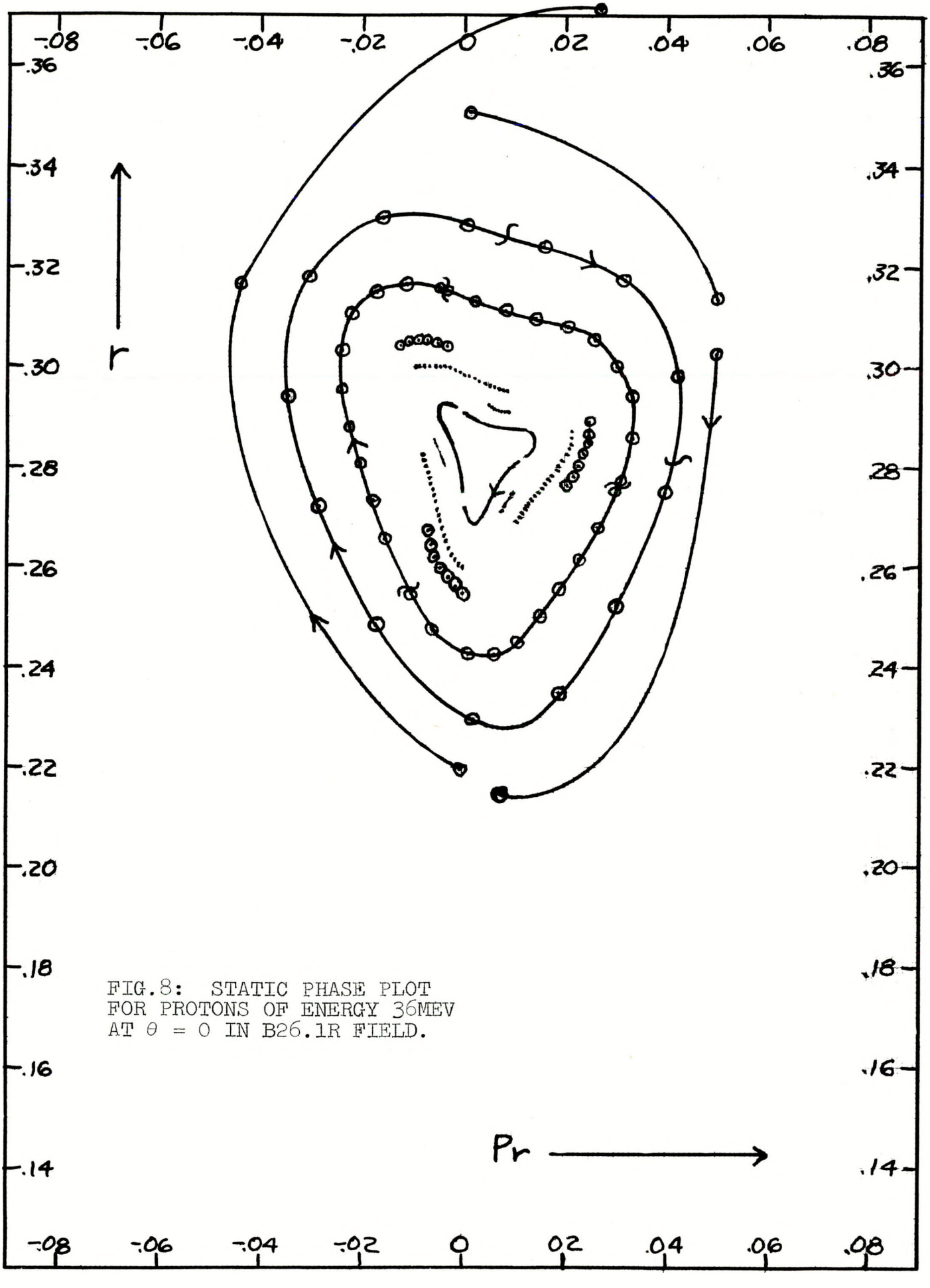

FIG.8: STATIC PHASE PLOT
FOR PROTONS OF ENERGY 36MEV
AT θ = 0 IN B26.1R FIELD.

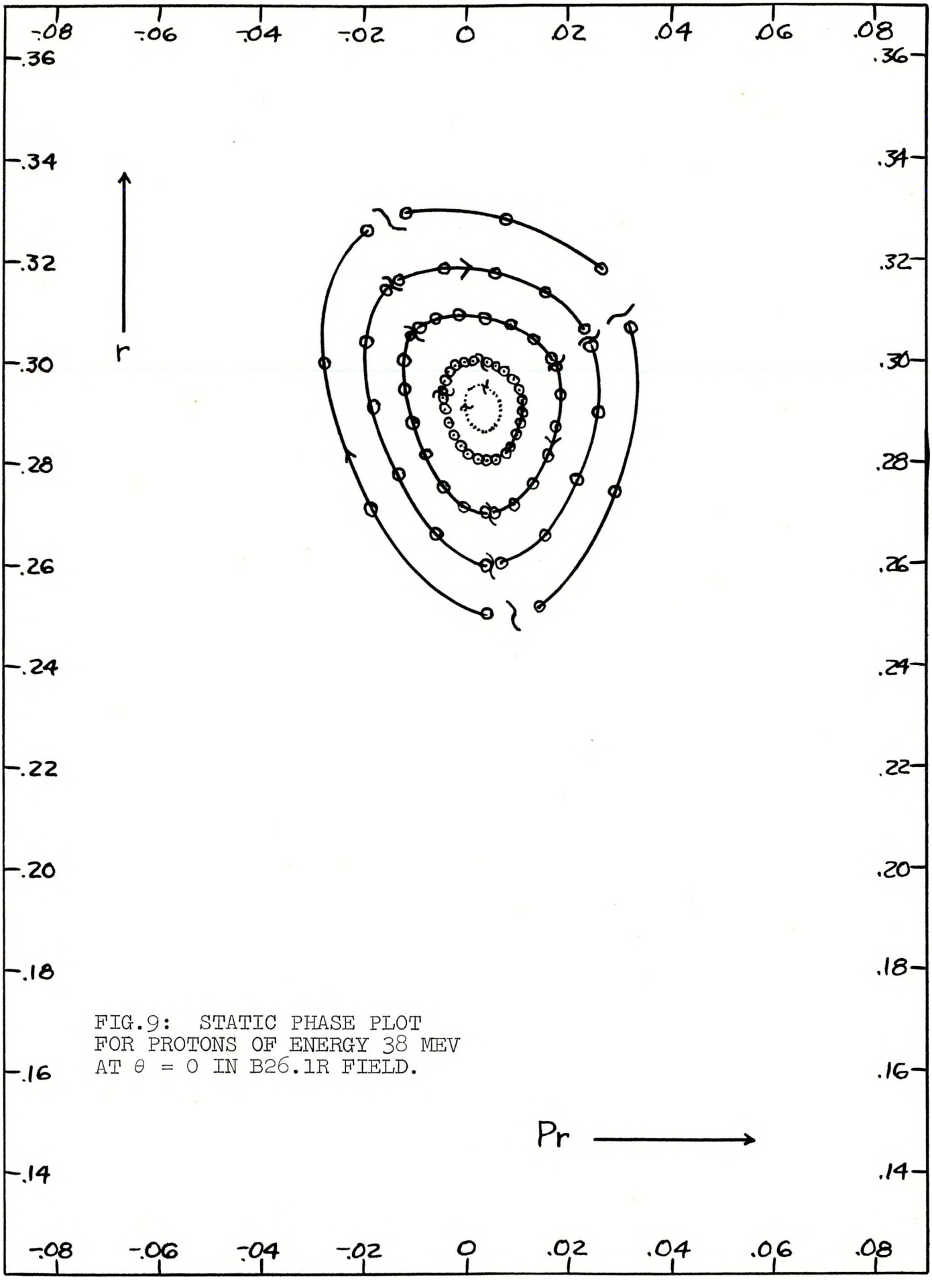

FIG.9: STATIC PHASE PLOT
FOR PROTONS OF ENERGY 38 MEV
AT θ = 0 IN B26.1R FIELD.

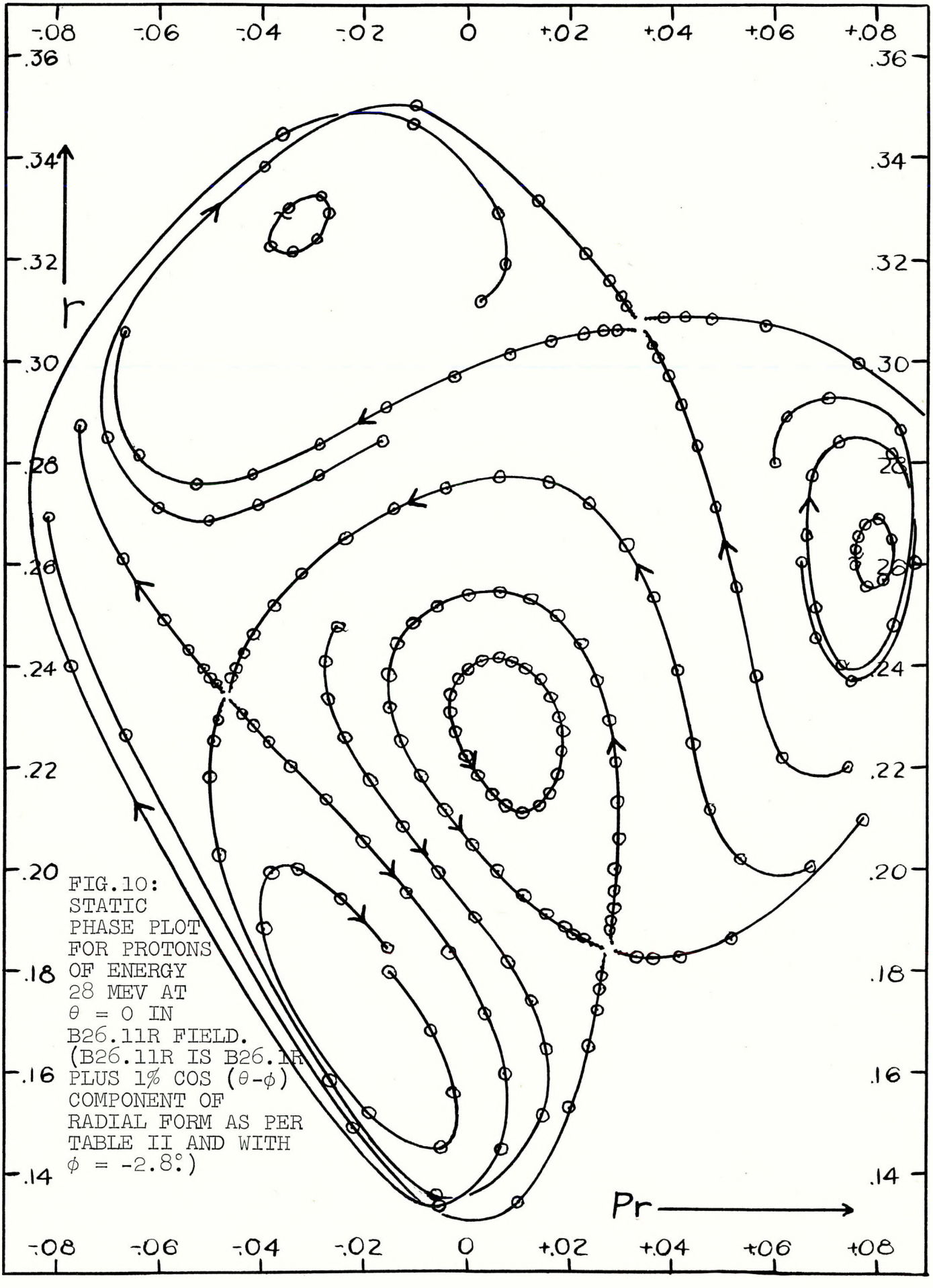

FIG.10: STATIC PHASE PLOT FOR PROTONS OF ENERGY 28 MEV AT $\theta = 0$ IN B26.11R FIELD. (B26.11R IS B26.1R PLUS 1% COS $(\theta-\phi)$ COMPONENT OF RADIAL FORM AS PER TABLE II AND WITH $\phi = -2.8°$.)

5. M. M. Gordon, MSUCP report, in preparation. A somewhat less general equation has been extensively treated by L. J. Laslett MURA 452, 459, 461, 463, 490, and 515, unpublished.

28 Mev phase plot analagous to Fig. 1 for the field with bump.[6] Four closed regions are still in evidence but now,

6. The powerful effect of a cos θ field component in a cyclotron ($\nu_r \simeq 1$) is clearly evidenced by the large changes in the phase plot which result when the small 1% bump is added. The results evedence the factors underlying the great respect assigned to such a field component in semi-empirical cyclotron design lore.

in addition, bands from the outer region weave in and around the various stable regions or in often used terminology the "corners" of the central region are said to have "opened". (In terms of the categorization set forth in MSUCP-6, the plot is a roughly equal mixture of one corner and two corner opening states as is seen by inspecting the trajectories starting in the vicinity of the three unstable fixed points.)

Fig. 11 is an r, p_r plot showing fixed point location versus energy as in Fig. 2, but for the field with bump. The fixed points again pair off and vanish leaving only a single point at high energies, but in a radically different way. E0 and U1 pair and vanish first followed by U2 and S3 and finally by U3 and S2. S1 remains at high energy. In effect, introduction of the field bump has caused a discontinuous jump in the location of the central stable orbit in the phase diagram -- at low energies this orbit is E0, at high energies it is S1. This is then the crux of the extraction process. A beam of particles initially near the equilibrium orbit will be dumped out and will eventually end up executing a very large amplitude oscillation about S1. The large amplitude

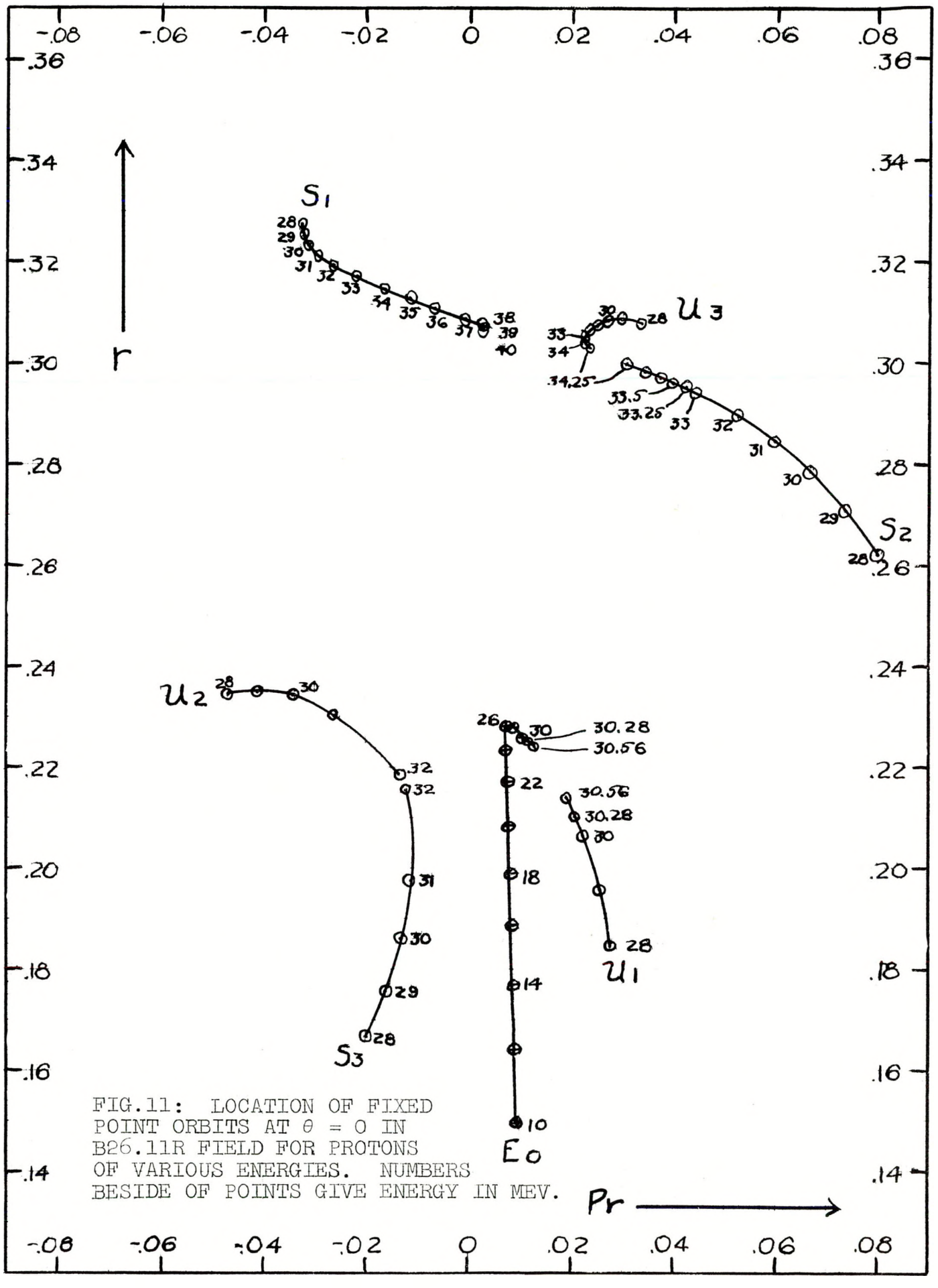

FIG.11: LOCATION OF FIXED POINT ORBITS AT θ = 0 IN B26.11R FIELD FOR PROTONS OF VARIOUS ENERGIES. NUMBERS BESIDE OF POINTS GIVE ENERGY IN MEV.

oscillation gives corresponding large change in beam position each turn which is the essential requirement for high efficiency extraction. Unfortunately the large amplitude oscillation also tends to take the beam into a strongly non-linear region which can lead to severe distortion as is considered in detail in the following section.

Figure 12 is a polar plot of 30 Mev fixed point orbits (with the field bump included) superimposed on the same approximate contour map as Figs. 3 and 4. Pairs of orbits are seen on careful inspection to be displaced toward each other, the equilibrium orbit being particularly close to one of the unstable fixed point orbits. The displacement of the equilibrium orbit is just as would be expected from introduction of a bump at -2.8° in an azimuthally symmetric field with positive k. The behavior of the unstable fixed point, cannot be inferred from such simple considerations.

Figs. 13 thru 17 are a set of static phase plots at the same energies as Figs. 5 thru 9 but with the bump included in the field. From comparison of corresponding figures the detailed effect of the bump at each energy can be seen.

IV. ACCELERATED ORBIT RESULTS

To determine the aberrations in an accelerated beam, an array of particles with definite geometrical arrangement in r, p_r space is traced thru successive revolutions with acceleration included -- changes in the geometry of the array reflect the distortions and aberrations of the system. Performance is good if the beam area remains in a shape which will fit conveniently into the apertures of subsequent lenses with no mixing of filled and empty regions of phase space. Since the apertures of lens, analyzing magnets, etc. are normally elliptical in phase space, the requirement is simply that a beam sized ellipse remain an ellipse, i.e. stretching and rotation are fine but not twisting, filamentation, etc.

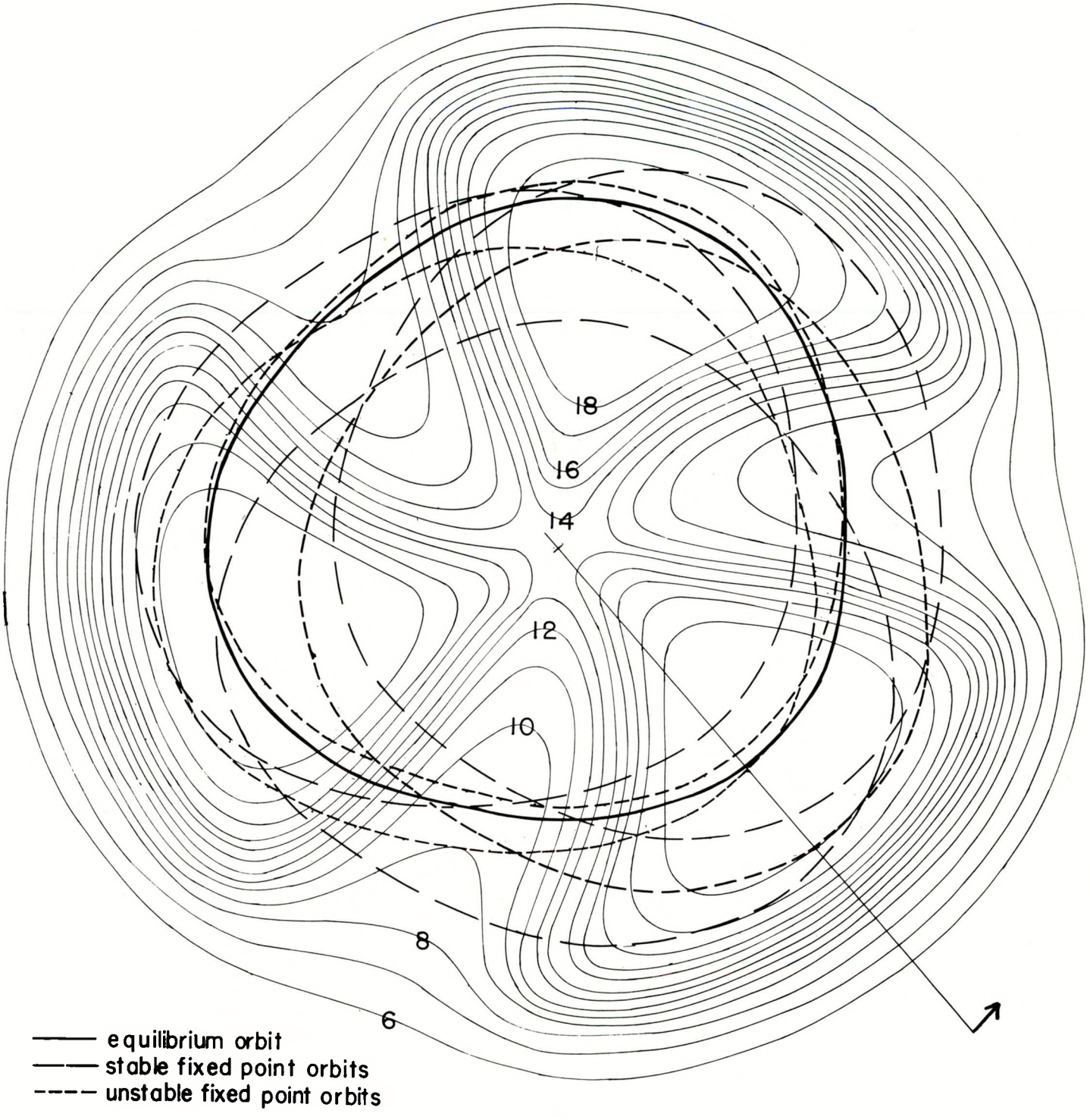

FIG.12: POLAR PLOT OF SEVEN FIXED POINT ORBITS FOR 30 MEV PROTONS IN B26.11R FIELD SUPERIMPOSED ON CONTOUR MAP OF RUN 26 FIELD. RADIAL LINE MARKS $\theta = 0$; FORWARD ROTATION IS IN DIRECTION OF ARROW. NUMBERS ON CONTOUR LINES GIVE FIELD STRENGTH IN KILOGAUSS.

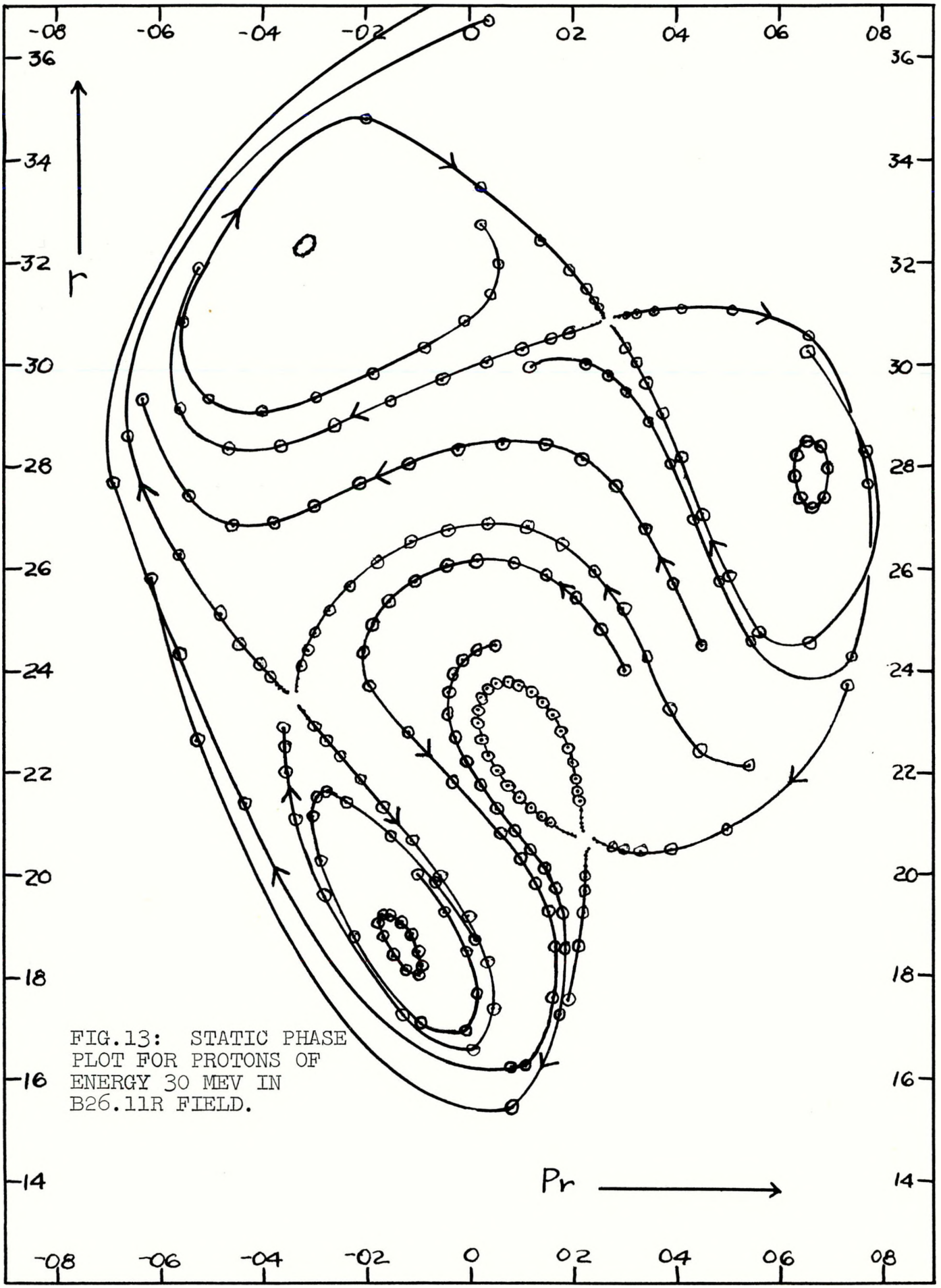

FIG.13: STATIC PHASE PLOT FOR PROTONS OF ENERGY 30 MEV IN B26.11R FIELD.

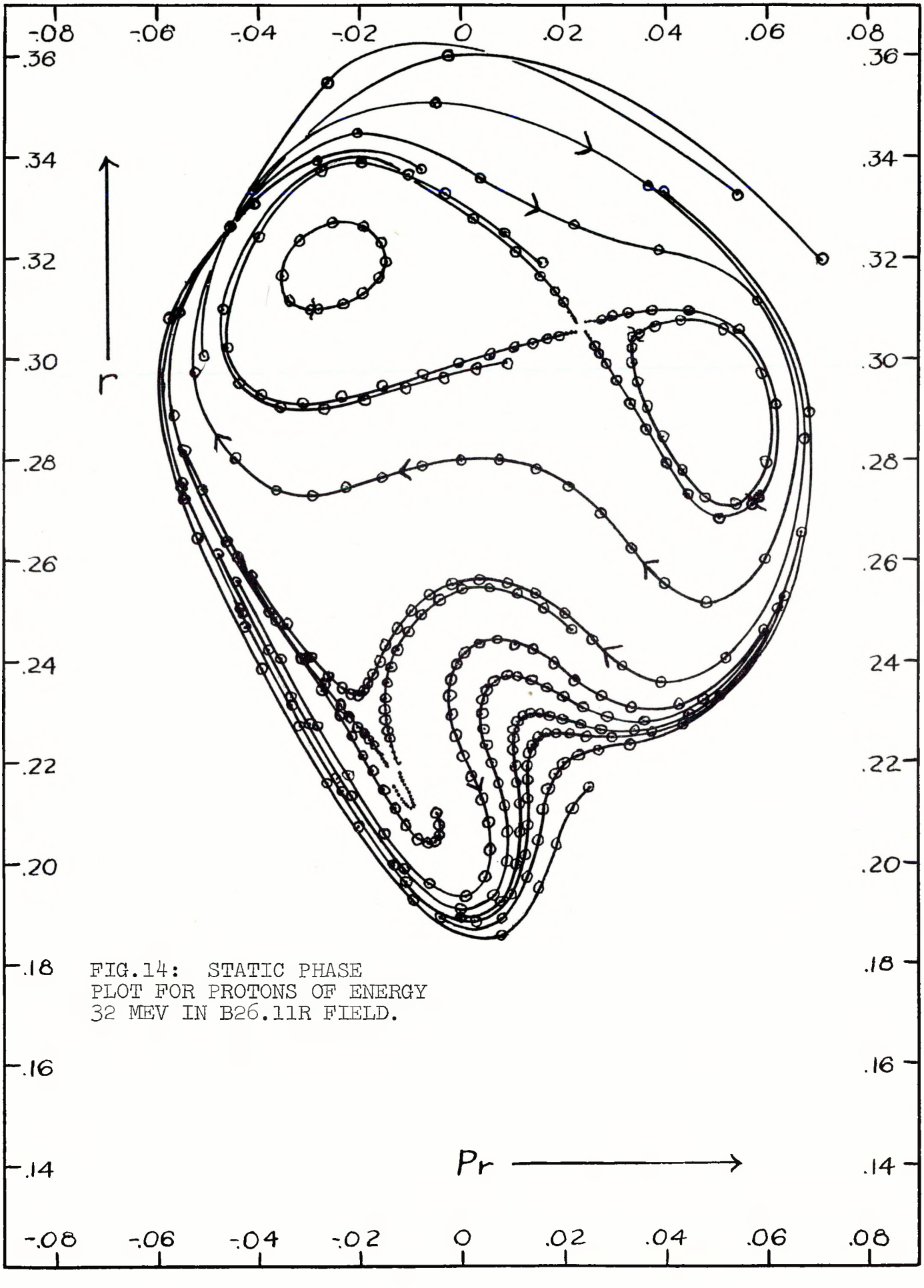

FIG.14: STATIC PHASE PLOT FOR PROTONS OF ENERGY 32 MEV IN B26.11R FIELD.

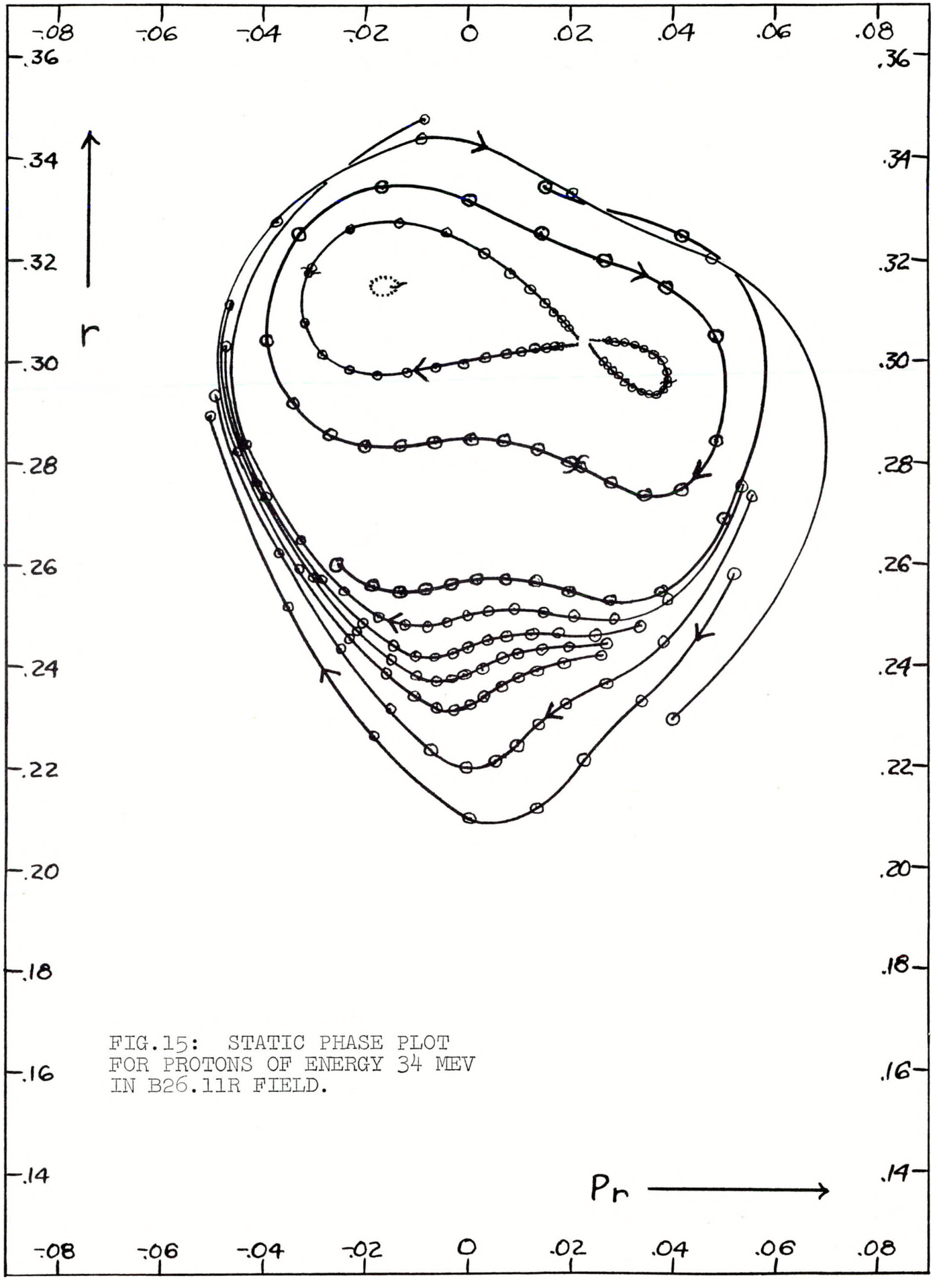

FIG.15: STATIC PHASE PLOT
FOR PROTONS OF ENERGY 34 MEV
IN B26.11R FIELD.

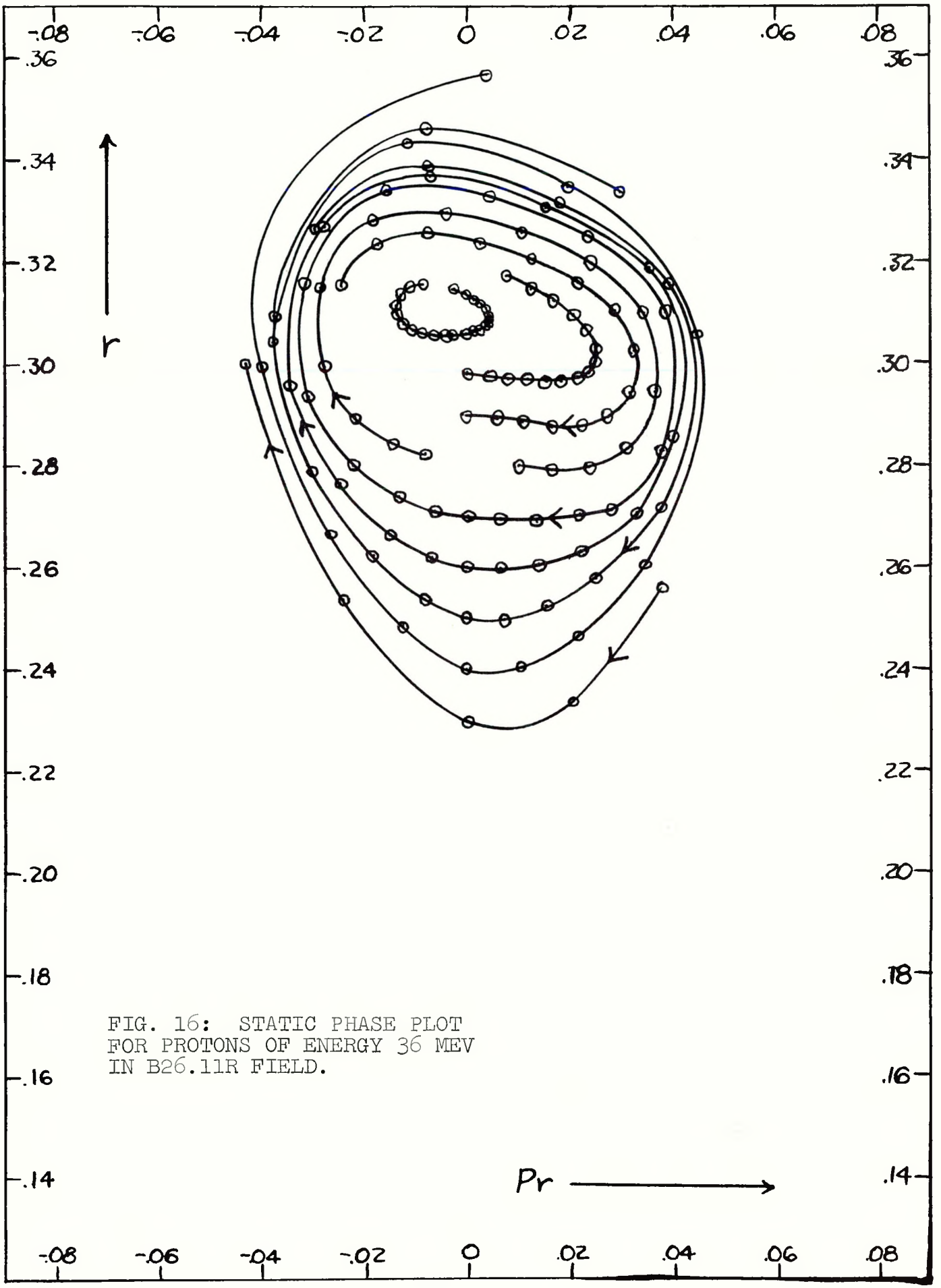

FIG. 16: STATIC PHASE PLOT FOR PROTONS OF ENERGY 36 MEV IN B26.11R FIELD.

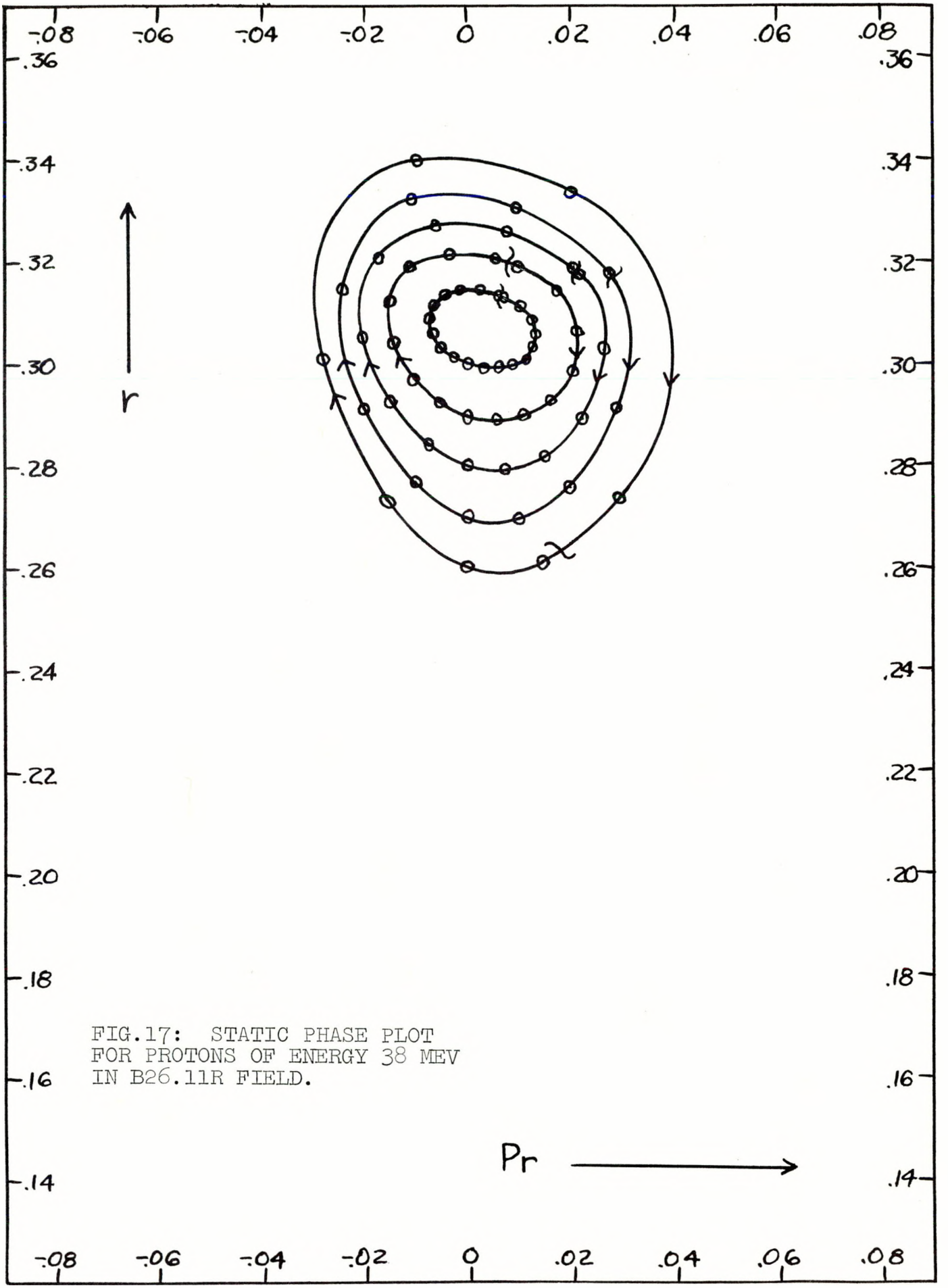

FIG.17: STATIC PHASE PLOT
FOR PROTONS OF ENERGY 38 MEV
IN B26.11R FIELD.

Fig. 18 is an r, p_r plot at $\theta = 0$ showing results from three sets of accelerated runs, starting initially in each case from a square array of outside dimensions .004 x .004 cyc. units. In the group labeled A the square is initially centered at r = .215 and p_r = -.005 and 5 particles, the four corner particles plus the center particle of the square, have been tracked. Group B is initially centered at r = .227 and p_r = +.011 and 24 orbits comprising all even quarter locations of the square except the lower right corner (the "notched" corner) have been tracked. Group C is initially centered at r = .226 and p_r = +.021 and 9 orbits comprising all even half locations of the square have been tracked. All three of the groups of particles start with an initial energy of 30 Mev and all are accelerated by an assumed square wave voltage of 280 kv/turn, the accelerating gaps being located at $\theta = 90°$ and 270°. The digits by each pattern in the figure give the number of completed revolutions. Since the voltage is a square wave, the energy of any group is simply 30 Mev plus 280 kev times the number of completed turns.

A good extraction system is one which yields large separation of successive turns[7]. and minimal amounts of the

---

7. The turn separation can be in any direction on the phase plot -- the features of the plot rotate as the azimuth at which the plot is made is changed and so a separation in any direction at $\theta = 0°$ will at some azimuth be a pure radial separation.

---

undesirable distortions discussed above. From the figure the extent of the undesirable distortions clearly depends on the size of the area under consideration. Small subareas of the patterns are much less distorted than the whole pattern. In a previous study,[8]. taking account of presently available

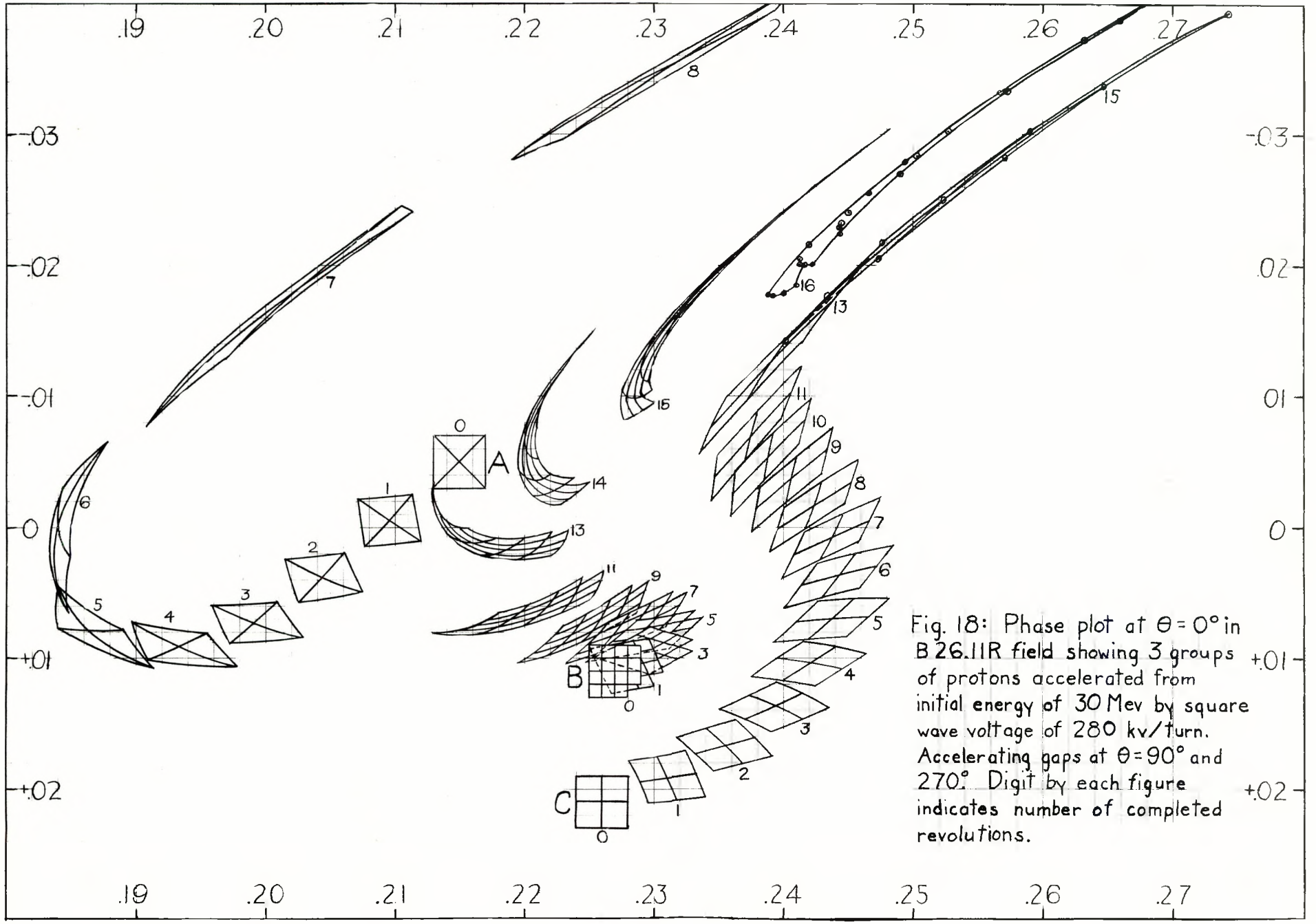

Fig. 18: Phase plot at $\theta = 0°$ in B 26.11R field showing 3 groups of protons accelerated from initial energy of 30 Mev by square wave voltage of 280 kv/turn. Accelerating gaps at $\theta = 90°$ and 270°. Digit by each figure indicates number of completed revolutions.

8. H. G. Blosser and M. M. Gordon, Performance Estimates for Injector Cyclotrons, Midwestern Universities Research Assoc. Report, No. 593 , (unpublished).

information on source luminosity, it was concluded that a beam with radial phase area equivalent to that of a circle of diameter .002 cyclotron units, would result in currents approaching the space charge limit.

Focusing attention then on .002 diameter subareas, the region near the notched corner of group B is clearly the best for extraction. Between the ~~13~~ 14th and ~~14~~ 15th turns a separation of .006 cyc. units is achieved with only moderate distortion. It is useful to try to understand the superior performance of this area in terms of features of the static phase plots, Figs. 13 thru 17.

First of all in this regard, recall that increases in the rate of motion of the beam spot on the accelerated phase plot (such as are necessary to induce turn separation adequate for extraction) arise from two basically different phenomena, one, the "static effect", arising from change in flow rate from one region to another of the applicable static phase plot, the other, the "acceleration effect", arising from the continual shifting of the applicable static phase plot as the particle energy increases.

Shifts in the rate of motion due to the static effect are almost entirely bad as can be seen by considering the motion of an area on a static phase plot. Undesirable features include:

1) The area stretches in proportion to the change in flow rate -- if turns initially overlap they will continue to do so no matter how rapid the flow rate becomes.

2) As the area stretches, curvature of the flow lines gives rise to bending of the area.

3) The gradient of the flow rate is seldom in the same direction as the flow, as is evidenced in the outer flow lines of Figs. 13 thru 17, so that shearing effects arise --

one side of the area moves faster than the other side.

4) The area may move into a disorganized region such as are indicated by the crisscross flow lines in several regions of the static plots -- filamentation will result.

The acceleration effect is in contrast, basically good. Consider a single gap crossing. Energy changes essentially instantaneously when the particle crosses the gap, and likewise the applicable static phase plot changes. There is however no change in either r or p_r (assuming radial accelerating gaps) and hence all geometrical features of the beam spot in phase space are preserved. If the applicable static phase plot at the after gap crossing energy has a higher flow rate than the one at the before gap crossing energy, the net effect is to put the beam in a region of higher flow rate without changing the geometry of the beam phase area which is clearly the desirable characteristic for a resonant extraction process.

An ideal extraction system, in fact, would be one in which the beam moved on entirely linear phase plots at all times but with the equilibrium orbit position shifted rather suddenly[9]. off center by a substantial amount so that a small

---

9. Suddenly as a function of energy -- say, in 1/2 of a radial precessional cycle or less.

---

amplitude oscillation would in a few revolutions become a large (but sill linear) oscillation about the displaced orbit. Provided the ν_r for the displaced orbit was sufficiently far from resonance, the resulting precessional motion of the beam would provide turn separation without distortion. Unfortunately, such a system appears to be self-contradictory. To suddenly jump the equilibrium orbit by a large amount requires rapid field shifts and hence, undoubtedly, substantial non-linearity.

Practical resonant extraction systems, in fact, appear to always involve substantial non-linearities. Optimization of such a system consists then, in programming the beam phase

area along a path which as nearly as possible avoids bad regions of the applicable static plots containing large flow rate gradients, such as the vicinity of an unstable fixed point for example. With this done, speeding up of the flow rate is as fully as possible a result of the acceleration changing the applicable phase plot and distortions are correspondingly minimized.

Looking again at Fig. 18 notice that Group C behaves nicely thru roughly the 11th turn (33.08 Mev) after which it suddenly stretches with great rapidity and with an actual reduction in turn separation. Figs. 14 and 15 make this behavior easily understandable. If the 7th turn (31.96 Mev) Group C pattern is superimposed on Fig. 14 the pattern is found to lie on flow lines headed directly for the U2 fixed point. U2 vanishes before Group C reaches its vicinity, but nevertheless a considerable slowing down of flow persists in the region as can still be seen at 34 Mev (Fig. 15), and, as noted, the energy of Group C is more nearly 33 Mev when crossing the bad region. From the 11th to the 13th turns, then, Group C is acted on by an extremely large gradient in the static flow rate -- hence, the static effect predominates and severe distortions ensue.

Group A fares better than Group C but nevertheless on the 6th and 7th turns moves into a region of rather high flow rate gradient (see Fig. 14) which stretches the Group rather badly. Finally the secret of Group B's success is due to the fact that its course across the phase diagrams eases it rather gradually into the rapidly moving outer region and so the static effects are minimized.

The results clearly indicate the desirable features of a static phase plot in so far as resonant extraction is concerned, namely, a minimum of change in flow rate on a static plot and a maximum of change in flow rate as the energy is changed. While certain comments relating these phase plot properties to field features could be made on the basis of results herein reported, it is deemed more appropriate, in

view of several studies in this regard presently in progress, to defer the topic to a later report.

From foregoing discussion it is clear that the extent of distortions in a resonant extraction system will depend sensitively on the voltage gain per turn. Raising the voltage advantages the acceleration effect, lowering it advantages the static effect. As a quantitative check on the sensitivity of the phenomena to changes in the voltage, the Group B particles from Fig. 18 were run two additional times with volts per turn of 1/2 and 2 times the Fig. 18 value. The results are shown in Fig. 19. In this figure, the group moving off to the right is being accelerated with 560 kev/turn, the group to the left with 140 kev/turn, and the group in the center is Group B. To avoid confusion the complete grid has been omitted on most of the early turns. One point from each of the runs has however been plotted on every turn and connected with a line. The 560 kev group is notably well behaved, in accord with expectation.

Another point of interest concerns the direction of rotation of the accelerated beam. In a spiral sector cyclotron it appears qualitatively clear that extraction will be easier if the beam rotates in a direction such that it tends to come off running along a valley of the field. The B26.1R field has a slight spiral and by chance all the results reported above are with the beam rotating in the opposite sense with respect to the spiral than is suggested by the qualitative argument. As an exploratory check on the effect, nine particles from Group B were accelerated rotating in the opposite direction. The results are shown in Fig. 20. The performance is slightly poorer although not markedly so. Since the spiral is quite weak, ($-60°$ per cyc. unit), the result is not surprising.

Fig. 21 presents results of a set of runs made for the purpose of checking quantitatively the effect of the unrealistic square wave accelerating voltage involved in all the previous accelerated runs. (The square wave was employed as a convenience in order to decouple E, t, and r, p_r phase space.) The Fig.

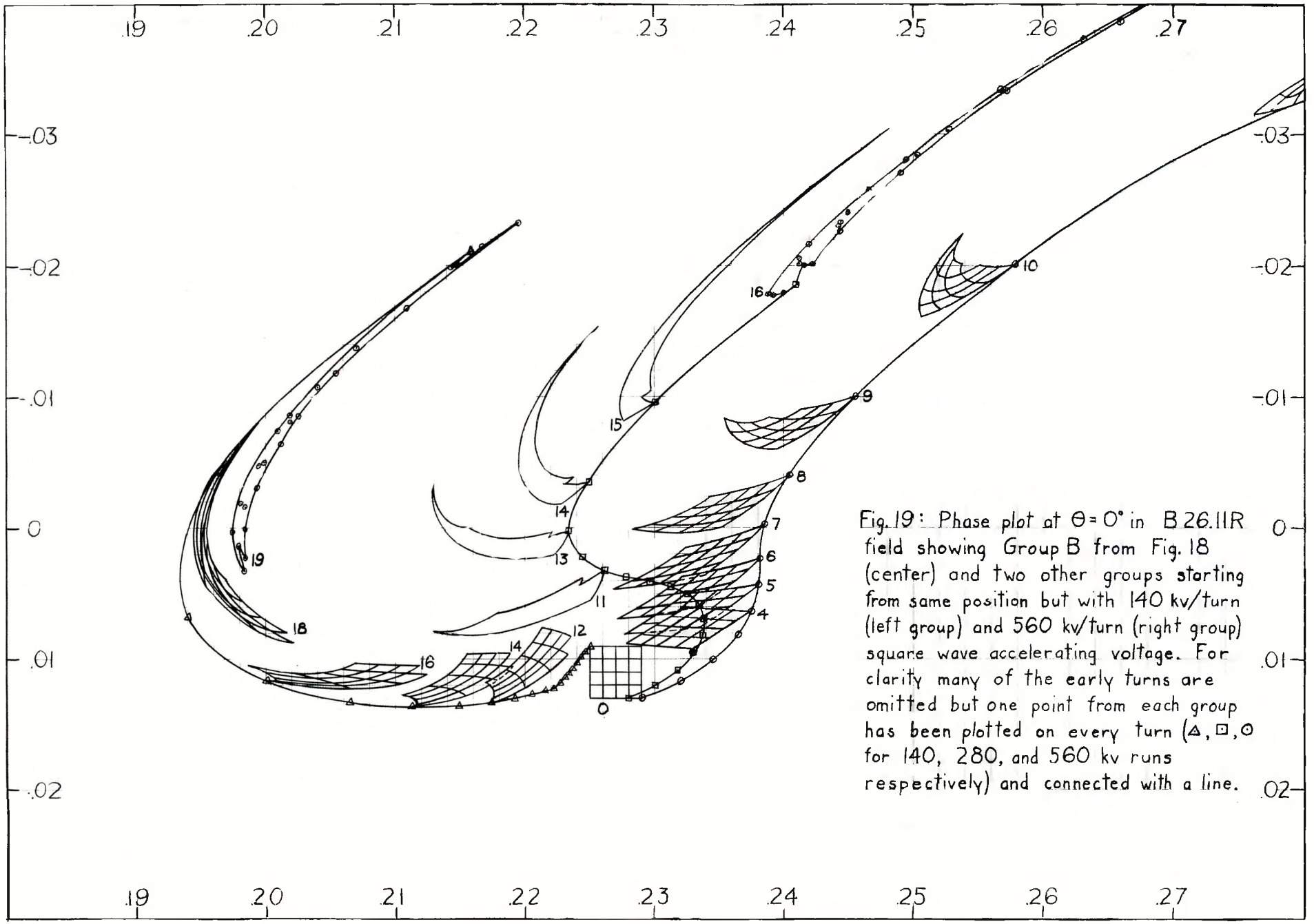

Fig. 19: Phase plot at $\theta = 0°$ in B 26.11R field showing Group B from Fig. 18 (center) and two other groups starting from same position but with 140 kv/turn (left group) and 560 kv/turn (right group) square wave accelerating voltage. For clarity many of the early turns are omitted but one point from each group has been plotted on every turn (△, □, ○ for 140, 280, and 560 kv runs respectively) and connected with a line.

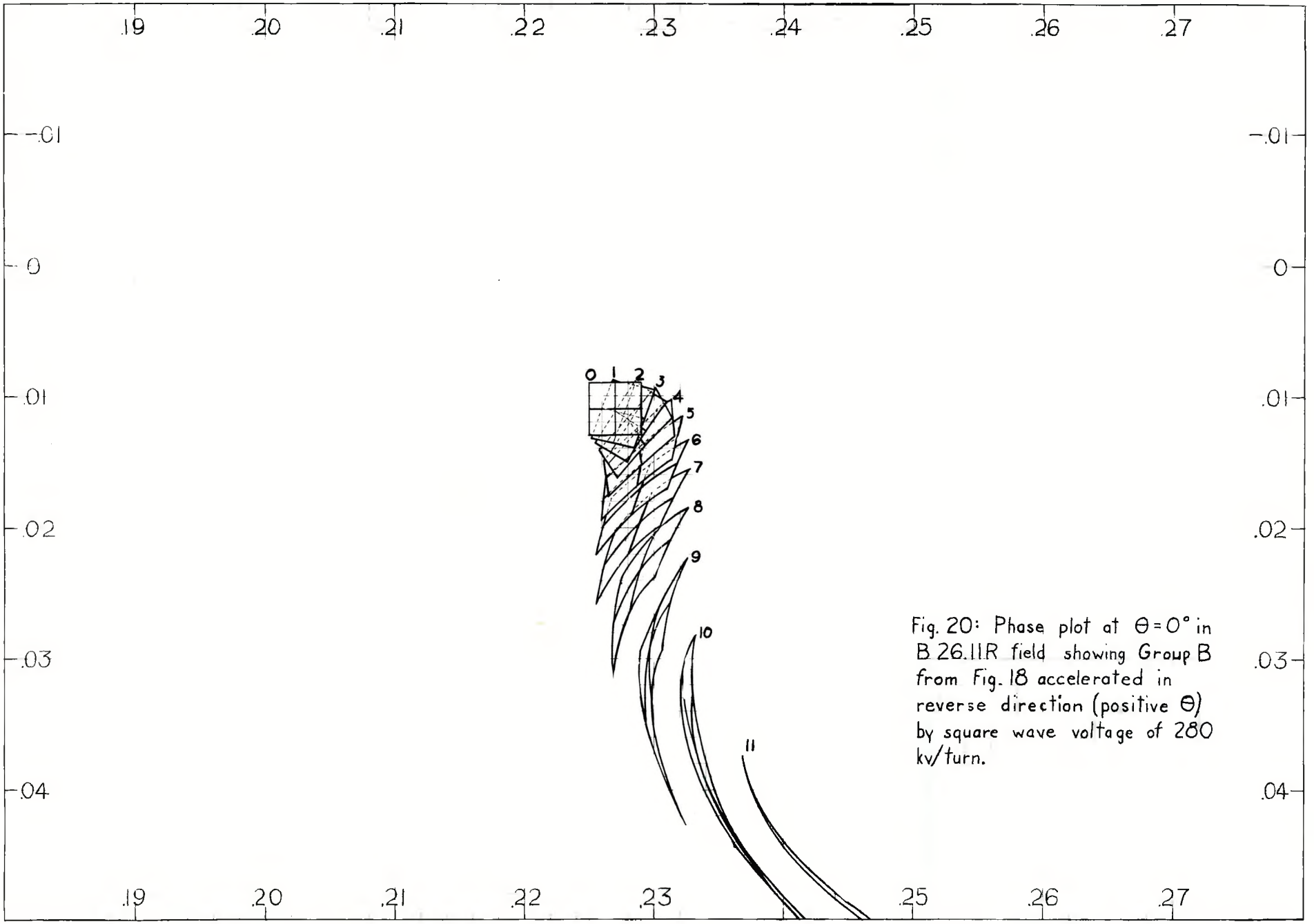

Fig. 20: Phase plot at $\theta = 0°$ in B 26.11R field showing Group B from Fig. 18 accelerated in reverse direction (positive θ) by square wave voltage of 280 kv/turn.

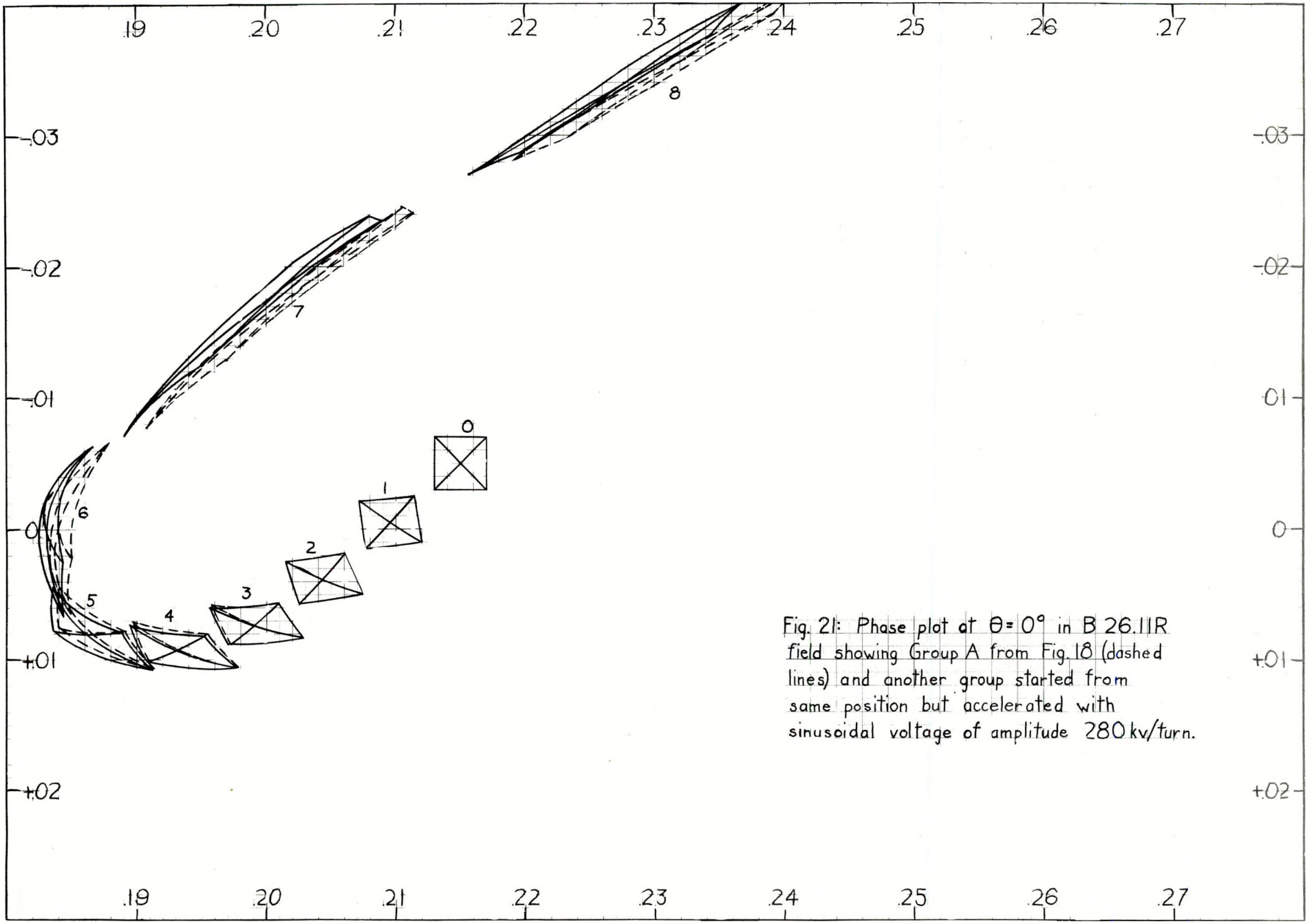

Fig. 21: Phase plot at $\theta = 0°$ in B 26.11R field showing Group A from Fig. 18 (dashed lines) and another group started from same position but accelerated with sinusoidal voltage of amplitude 280 kv/turn.

shows results of a rerun of Group A of Fig. 18 with sinusoidal voltage. For comparison the square wave results are also shown being represented by the dashed line in the Figure. The sinusoidal voltage, it is seen, shifts the final position of the beam spot but has almost no effect on the distortion. An energy spread is also introduced due to differential phase slip; at the end of the 8th turn, the total energy spread for the 5 particles was 62 kev and the average total drift in phase was 55° (the runs started with particles and voltage in phase). The energy spread across a beam sized subarea would be roughly 30 kev. Group A moves in a more non-isochronous region of the magnet than either Group B or Group C of Fig. 18. It makes fewer turns however and actually the final total phase slip of all three groups is approximately the same. Shifting from the square wave to sinusoidal voltage should therefore have equivalently minor effect on the other groups.

A final phenomena worthy of comment concerns the initial direction of motion of Group B in Fig. 18. Fig. 22 shows this Group after 0, 1, and 2 revolutions superimposed on static phase plots for the three energies.[10.] The group is seen to move off

---

10. Note that both Groups A and C from Fig. 18 are well outside the stable region initially as is clear from comparison with Fig. 22. Below 30 Mev the stable region enlarges quite rapidly as is seen from Fig. 11 and actually a sampling of backward deacceleration runs shows that both A and C are in the stable region at lower energies.

---

at approximate right angles to the direction of flow of the static plots. The curious effect is an example of a phenomena called the gap crossing resonance by Gordon and treated by him.[11.]

---

11. M. M. Gordon, private communication, (to be published).

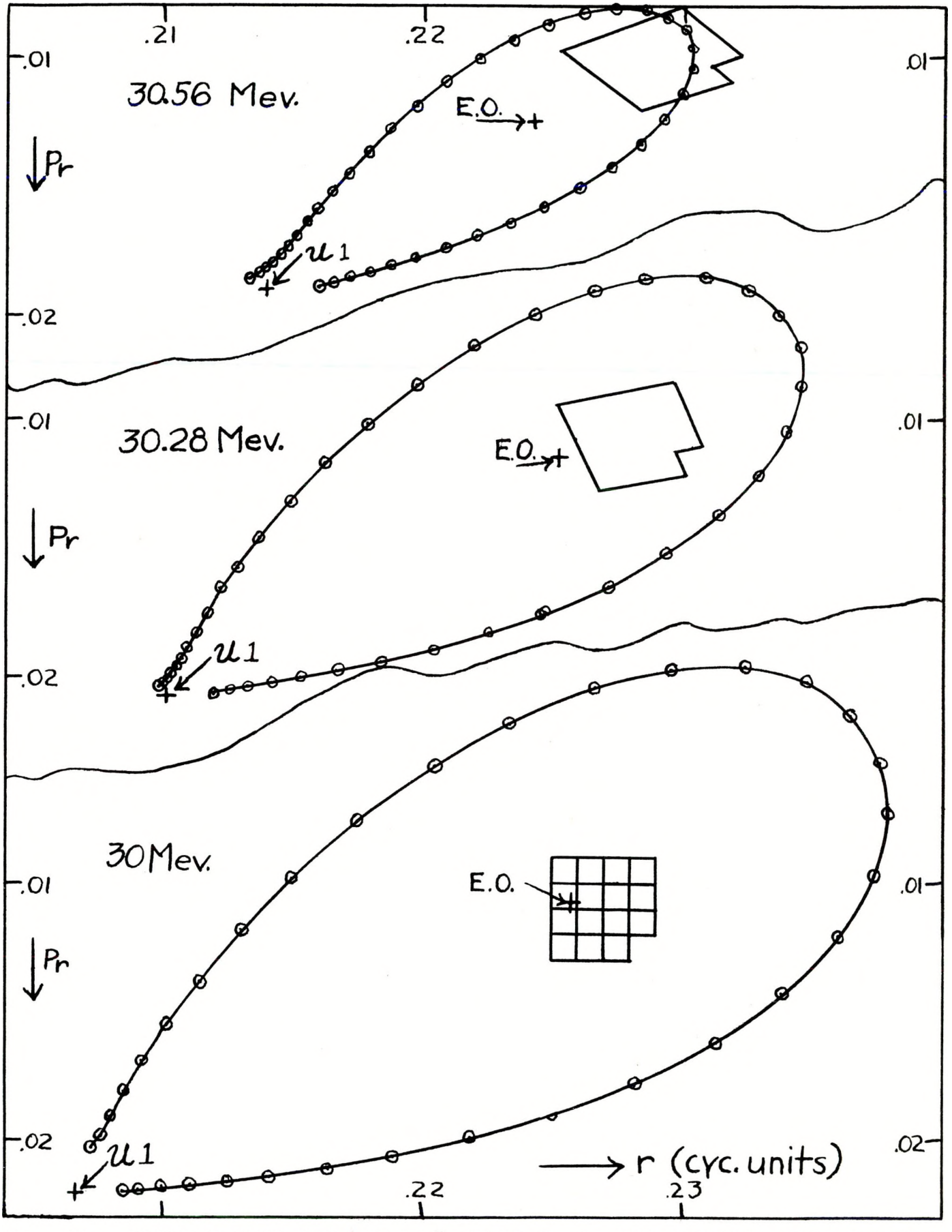

FIG.22: GROUP B GRID FROM FIG.18 AFTER 0, 1, AND 2 TURNS SUPERIMPOSED ON STATIC PHASE PLOTS FOR RESPECTIVE ENERGIES. ON 3RD AND SUCCEEDING TURNS NO STABLE REGION REMAINS.

The phenomena can also be thought of as a special form of r-f knockout.[12] From either point of view, the particular

---

12. K. M. Terwilliger, (private communication).

---

behavior of Group B is readily understandable. Consider for example the point in the Group B area which at 30 Mev and $\theta = 0$ is exactly on the equilibrium orbit. This particle will remain on the equilibrium orbit to $\theta = 90°$, at which point its energy changes to 30.14 Mev. The equilibrium orbit for 30.14 Mev will be at a different location in the r, p_r space from that at 30.00 Mev -- since the particle's r, p_r is unchanged by the acceleration, an amplitude is generated. Referring to Table III, the spacing of 30.28 and 30.0 Mev equilibrium orbits is given at several θ's. Interpolating with respect to energy, the particle's amplitude immediately after the gap crossing is inferred to be .00126 cyc. units and in the direction $\phi = 138°$ (the particle's amplitude is the negative of the equilibrium orbit shift) where the orientation of ϕ is as stated in the Table III caption. Using the Table III data on the behavior of the two displaced 30 Mev orbits to determine a linear mapping from 90° to 270°, and assuming the 30 Mev mapping is the same as that for 30.14 Mev, the A of .00126 and the ϕ of 138° at $\theta = 90°$ are found to change to .00095 and -23° as the particle moves to $\theta = 270°$. At 270° the energy again jumps generating an additional amplitude (from Table III) of magnitude .00084 and direction 253° which adds vectorially to the incoming amplitude, yielding a resultant total amplitude after the gap crossing of magnitude .00133 and direction -62°. Again using the two results for the displaced 30 Mev orbits, the mapping from 270° to 360° can be inferred yielding an estimated final amplitude of .00161 and a ϕ of 28° at the end of the turn. Comparing with the Fig. 22 plot at the end of the turn (30.28 Mev), the result is seen to fairly accurately predict the actual amplitude and ϕ of this point of the grid (i.e. the location,

θ	E.O. 30.28 to E.O. 30.0		X_1 30.0 orbit to E.O. 30.0		X_2 30.0 orbit to E.O. 30.0	
	A	ϕ	A	ϕ	A	ϕ
0°	.000826	-128.6°	.001000	0°	.001000	-90°
90°	.002526	-42.1°	.000910	90.7°	.001104	-4.6°
270°	.001684	+72.6°	.000996	273.7°	.001120	210.2°
360°	.000826	+231.4°	.001129	370.3°	.000921	296.4°

Table III: Separation at θ = 0°, 90°, 270° and 360° of: (1) 30.28 and 30.0 Mev equilibrium orbits (2) 30.0 Mev E.O. and orbit displaced in r direction and (3) 30.0 Mev E.O. and orbit displaced in p_r direction. Separation is given as amplitude and phase with ϕ = 0 in direction of increasing r and with positive rotation being toward $-p_r$ direction.

relative to the grid structure, which at $\theta = 0$ on the previous turn was exactly on the equilibrium orbit).

The behavior of any other point in the grid can be similarly estimated by noting that such a point differs from the one considered simply by an additive amplitude vector; this additive vector, in passing thru the turn, will rotate and change in length by an amount which to good accuracy can be inferred from the static phase plot. Since the same statement can be made about every point of the figure, the net result is a rotation and stretching of the figure about the above considered 30 Mev E.O. point, the amount of the rotation and stretching being proportional to the spacing and amplitude of the points on the static phase plot with respect to the equilibrium orbit. Since points on the static plot above and below the equilibrium orbit move thru a greater angle than those to right or left, vertical lines in the beam spot rotate more than horizontal lines giving the skewing effect observed.

Note, in this example, that the major contribution to the generated amplitude comes from the fact that the equilibrium orbit spacings at the two gaps are nearly in opposite directions in the phase space so that their contributions to the amplitude are additive. This could clearly not occur if the field had 180° symmetry. (The difference in E.O. spacing is the correction mentioned in a previous section, which must be taken into account in inferring accelerated orbit behavior in the present field from full turn static phase plots rather than from half turn mappings. Note that away from the neighborhood of fixed points even this correction is negligible, since only near a fixed point does the direction and rate of flow in the phase space depend sensitively on the exact amplitude.)

V. CONCLUSIONS

The numerical results of the previous section demonstrate that with care and adequate volts per turn resonant extraction

systems with excellent optical characteristics can be realized. The essential design requirement of such a system is a turn program which avoids regions of large flow rate gradient in the static phase space. Results with respect to both turn separation and distortion are quite sensitive to the volts per turn. For the MSU design in particular it is clear that volts per turn substantially lower than the designed 280 kev/turn would result in sharp reduction of both extraction efficiency and optical quality.

In contrast with the qualitative ideas set forth in MSUCP-2,[13.] the present results show that beams entering the extraction region approximately centered on the equilibrium orbit behave as well or better than beams entering with substantial displacement.[14., 15.]

13. H. G. Blosser and M. M. Gordon, Proposal for Study of a Resonant Extraction System, Nov. 1959, unpublished.

14. This result is in accord with qualitative anticipations of R. S. Bender (private communication).

15. Note that the field used herein is only slightly different from that in MSUCP-2 (smoothing and isochronizing) and that Group A of Fig. 18 is essentially the same as the group considered in said report.

VI. ACKNOWLEDGEMENTS

It is a pleasure to acknowledge the invaluable assistance of Miss Thelma Arnette in handling a number of matters related to the computer routines, of Mrs. Sue Bouck in the preparation of the manuscript, and of Mr. William Small in the preparation of the figures.